

FINAL CONTRACT REPORT

**INFLUENCE OF THE NEW LRFD SEISMIC GUIDELINES
ON THE DESIGN OF BRIDGES IN VIRGINIA**

**M.A. Widjaja
Graduate Research Engineer**

**C.L. Roberts-Wollmann, Ph.D., P.E.
Assistant Professor**

**Via Department of Civil and Environmental Engineering
Virginia Polytechnic Institute and State University**

Project Manager

Michael C. Brown, Ph.D., P.E., Virginia Transportation Research Council

Contract Research Sponsored by
Virginia Transportation Research Council

Virginia Transportation Research Council
(A Cooperative Organization Sponsored Jointly by the
Virginia Department of Transportation and
the University of Virginia)

Charlottesville, Virginia

March 2004
VTRC 04-CR17

NOTICE

The project that is the subject of this report was done under contract for the Virginia Department of Transportation, Virginia Transportation Research Council. The contents of this report reflect the views of the authors, who are responsible for the facts and the accuracy of the data presented herein. The contents do not necessarily reflect the official views or policies of the Virginia Department of Transportation, the Commonwealth Transportation Board, or the Federal Highway Administration. This report does not constitute a standard, specification, or regulation.

Each contract report is peer reviewed and accepted for publication by Research Council staff with expertise in related technical areas. Final editing and proofreading of the report are performed by the contractor.

Copyright 2004 by the Commonwealth of Virginia.

ABSTRACT

The Virginia Department of Transportation (VDOT) is currently using the *AASHTO Standard Specifications for Highway Bridges*, with some modifications, for its seismic highway bridge design. In April 2001, the *Recommended LRFD Guidelines for the Seismic Design of Highway Bridges* were published. To be prepared for the transition from the *Standard Specifications* to the *LRFD Guidelines*, VDOT must have an understanding of the impact of the new *LRFD Guidelines* on the cost for design and construction of Virginia bridges.

The influence of the *LRFD Guidelines* on Virginia bridges was investigated by analyzing two existing bridges. The first bridge has prestressed concrete girders and is located in the Richmond area. The second bridge has steel girders and is located in the Bristol area. Both bridges were two-span overpass structures with integral abutments. The bridges were analyzed using the methods prescribed in the guidelines. Then the combined effects of the dead, live and earthquake loads were compared to the strengths of the columns and the pier caps. The details of the bridge designs were also checked with the corresponding seismic design requirement.

Results indicate that typical column spiral reinforcement is not adequate to satisfy the requirements of the new seismic guidelines. For the bridge in the Richmond area, spiral reinforcement was increased from a No. 5 at a 5-in pitch to a No. 5 at a 4-in pitch. For the bridge in Bristol, the increase was greater, from a No. 3 at a 10.5-in pitch to a No. 5 at a 4-in pitch. In addition to the increase in spiral reinforcement, other details such as beam-column joint reinforcing and splice locations required modifications. The calculated cost increases for the two bridges were 0.1% and 0.3%.

In addition, a parametric study was performed to explore the effects on substructure design of different column heights, superstructure lengths and soil classifications in different parts of Virginia. The study indicated that for bridges located on good soil (Class B) typical column longitudinal reinforcing ratios (~1.5%) provide adequate strength to resist seismic forces. For bridges on poor soils (Class D) in regions of low to moderate seismic activity, column longitudinal reinforcing may need to be increased, particularly in bridges with short columns, long spans, and sliding bearings at the abutments. For bridges on poor soils in regions of higher seismic risk (south-western Virginia), column sizes may need to be increased. For columns designed as spiral columns the increases in transverse column reinforcement will not be great, but for columns designed as tied columns, the increases will be significant.

FINAL CONTRACT REPORT

INFLUENCE OF THE NEW LRFD SEISMIC GUIDELINES ON THE DESIGN OF BRIDGES IN VIRGINIA

M.A. Widjaja
Graduate Research Engineer

C.L. Roberts-Wollmann, Ph.D., P.E.
Assistant Professor

**Via Department of Civil and Environmental Engineering
Virginia Polytechnic Institute and State University**

INTRODUCTION

The Virginia Department of Transportation is currently using the *AASHTO Standard Specifications for Highway Bridges* (AASHTO 1996)(to be referred to for the remainder of this report as the *Standard Specifications*), with some modifications, for its seismic highway bridge design. In April 2001, the *Recommended LRFD Guidelines for the Seismic Design of Highway Bridges* (MCEER 2001)(to be referred to for the remainder of this report as the *LRFD Guidelines*) were published. The impact of the new guidelines on the design of bridges will vary from district to district within Virginia. In some districts the seismic requirements become more stringent, while in other districts the seismic requirements become less stringent. For the districts with more stringent seismic requirements, the resulting column longitudinal and confining reinforcement and pier cap beam reinforcement may need to be increased compared to designs using the *Standard Specifications*. To be prepared for the transition from the *Standard Specifications* to the *LRFD Guidelines*, VDOT must have an understanding of the impact of the new *LRFD Guidelines* on the cost for design and construction of Virginia bridges.

PURPOSE AND SCOPE

This project was initiated to assist VDOT in the evaluation of the proposed LRFD seismic guidelines. Specifically, the design modifications, level of design effort and increases in bridge costs were of interest. To evaluate the influence of the new *LRFD Guidelines* on the design of bridges in Virginia, the following specific objectives were established:

- Perform a critical comparison of old and new seismic provisions and identify expected changes for Virginia.
- Assess the required level of design effort using the new guidelines.
- Determine resulting design modifications required by the new guidelines on two previously designed bridges.
- Perform parametric studies on simple bridge configurations to evaluate the economic impact of the new design procedures on bridges in Virginia.

Initially a full review of old and new seismic design procedures was undertaken. Various aspects of the guidelines were assessed to determine the general impact on Virginia bridges.

To further assess the effects of the *LRFD Guidelines*, two previously designed bridges were evaluated for compliance with the *LRFD Guidelines*. One bridge had prestressed concrete girders and was located in the Richmond District, which is in Seismic Performance Category B under the *Standard Specifications*. The second had steel girders and was located in the Bristol District, which is in Seismic Performance Category A under the *Standard Specifications*.

Finally, a parametric study was performed on typical two-span bridge configurations to study the economic impacts of the new guidelines in terms of quantities of longitudinal and transverse steel in the columns. Many combinations of pier height and span length were investigated for three locations within the state and two soil classifications.

METHODS

Comparison between the *LRFD Guidelines* and the *AASHTO Standard Specifications*

The comparison of the *LRFD Guidelines* and the *Standard Specifications* was carried out by performing a point-by-point examination of the two seismic design approaches. The classifications of bridges, the determination of equivalent static seismic lateral forces, and other aspects of design were compared on a qualitative level. No quantitative comparisons were made in this portion of the study. The complete point-by-point comparison is detailed in the RESULTS section of this report.

Evaluation of Two Previously Designed Bridges for Compliance with *LRFD Guidelines*

Two previously designed bridges were evaluated for compliance with the *LRFD Guidelines*. The first bridge was the bridge on Woolridge Road over Rt. 288 in Chesterfield County. It was a two-span overpass structure with prestressed bulb-T girders, which was designed based on the 16th Edition of the *Standard Specifications* with 1997 and 1998 interims and VDOT Modifications. The second example was the pair of bridges on Rt. 19 over the connection of existing Rt. 19 in Tazewell County. These two bridges were also two-span overpass structures, but had steel plate girders, and were designed using the 14th Edition of the *Standard Specifications* with 1989, 1990, and 1991 interims and VDOT Modifications. For the three bridges, the new seismic design procedures were followed and the existing details were examined to determine how the bridge designs should be altered to bring them into compliance with the new seismic recommendations.

Typical Seismic Design Procedure for Virginia Bridges

This section outlines the procedure followed for the evaluation of the example bridges. The complete description of the process for each bridge is presented in the RESULTS section of this report.

To begin the seismic design of a bridge, the Spectral Acceleration curve must be generated. From the soil profile type and the location of the bridge, the Seismic Hazard Level can be determined. Then with an expected level of performance (life safety or operational), the Seismic Design and Analysis Procedure (SDAP) can be determined. The six different SDAPs are:

1. SDAP A1 and A2, for which no dynamic analysis is required.
2. SDAP B, which does not require a seismic demand analysis but requires capacity design principles and minimum design details
3. SDAP C, which combines a demand and capacity analysis, including the effect of inelastic behavior of ductile earthquake resisting elements. This SDAP can only be applied to bridges that behave essentially as a single degree-of-freedom system.
4. SDAP D, which is a one step design procedure using an elastic (cracked section properties) analysis.
5. SDAP E, which requires an elastic (cracked section properties) response spectrum analysis for the governing design spectra (50% Probability of Exceedance in 75-year or 3% Probability of Exceedance in 75-year/1.5 mean deterministic) and P- Δ design check.
(MCEER 2001).

For Virginia, the area with the highest seismic spectral accelerations is the southwestern part of the state, where Bristol is located. In a worst-case scenario, bridges located in the Bristol area that sit on poor soil are typically classified as Seismic Hazard Level III. Therefore the bridges with an operational level of performance in the Bristol area can use SDAP C, D or E. The two bridges analyzed in this study use SDAP D. The steps taken in this method are summarized as follows:

1. Calculate the material and section properties of the bridge and model it in RISA 3D (or similar three-dimensional frame solver).
2. Apply the dead and live loads to determine the axial forces in the columns.
3. Calculate the effective section properties of the columns.
4. Calculate the effective section properties of the pier cap beam.
5. Adjust the model to reflect the effective section properties.
6. Calculate the period of vibration of the bridge using the uniform load method or the single mode spectral analysis method.
7. Calculate the equivalent earthquake forces for the bridge using the uniform load method or the single mode spectral analysis method.
8. Apply the equivalent earthquake forces obtained from either method and calculate the effects of earthquake forces using the appropriate Base Response Modification factors (R factors).
9. Combine the effects of the earthquake, dead and live loads.
10. Check the columns and pier cap beams to determine if they have adequate flexural and shear strength to carry the combined effects of the earthquake, dead and live loads.
11. Compare the bridge details with the detailing requirements of the *LRFD Guidelines*.

This type of rigorous design procedures will require approximately 80 to 100 personnel hours, compared to merely a few hours to perform the calculations of the design criteria required by the *Standard Specifications* for the majority of Virginia Bridges.

Parametric Study

A parametric study was performed to evaluate the changes in longitudinal and transverse reinforcement required in typical bridge substructures for the *LRFD Guidelines*. A typical superstructure and substructure were selected, and the column height and the span length were varied. The substructure selected was a three column bent with 36 in diameter columns. The column heights evaluated were 20 ft, 30 ft, and 40 ft. The bridge comprised two spans, and the superstructure cross-sectional properties were based on a typical 50 ft bridge width. The span lengths varied from 80 ft to 140 ft. For each combination of column height and span, the fundamental period of vibration was determined. The spectral acceleration curves were developed for the bridge founded on two soil classes, B and D, and located in three different parts of Virginia:

1. Northern Virginia, which has relatively low seismicity,
2. the Richmond area, which has a moderate seismicity,
3. the Bristol area, which has the highest seismicity in the Commonwealth.

For each span length, column height and soil class combination in each region of the Commonwealth, the equivalent lateral earthquake forces were determined and applied to the bridge in combination with dead and live loads. Then the shears, axial loads and moments in the columns were calculated. Based on the force effects, the required longitudinal and transverse reinforcement ratios were determined and compared to typical designs. The complete process is outlined in the RESULTS section of this report.

RESULTS

Comparison of the *LRFD Guidelines* and the *AASHTO Standard Specifications*

This section describes some of the major changes between the *Standard Specifications*, Seismic Design Methods and the *LRFD Guidelines*. The major differences between the *LRFD Guidelines* and the *Standard Specifications* are as follows:

New USGS (United States Geological Survey) Maps

The *Standard Specifications* currently use a probabilistic map of peak ground acceleration (PGA) on rock, which is shown in Figure 1. The map by the USGS was published in 1990 (USGS 2002). The map shows the contours of PGA with a probability of exceedance of 10% in 50 years. The figure also shows the nine districts of VDOT. According to the *Standard Specifications*, all regions with a PGA greater than 9%g fall into Seismic Performance Category B. Those regions with lower PGA are Category A.

On the other hand, the *LRFD Guidelines* illustrate an updating of the ground motion maps, and give elastic response spectral accelerations for different periods of vibration. The two maps used by the *LRFD Guidelines* are the 0.2-second and 1.0-second spectral acceleration maps, which both have 2% probability of exceedance in 50 years. The maps are shown in Figures 2 and 3.

New Spectral Shapes

The response spectrum curve in the *Standard Specifications* has a maximum spectral acceleration for short periods, which are less than approximately 0.33 second, and decays at a rate of $1/T^{2/3}$ for longer periods, where T is the period of vibration in seconds. The *Standard Specifications* response spectrum curve is shown in Figure 4. The response spectrum curve in the *LRFD Guidelines* decays at a rate of $1/T$ and has smaller spectral accelerations for very short periods, as shown in Figure 5.

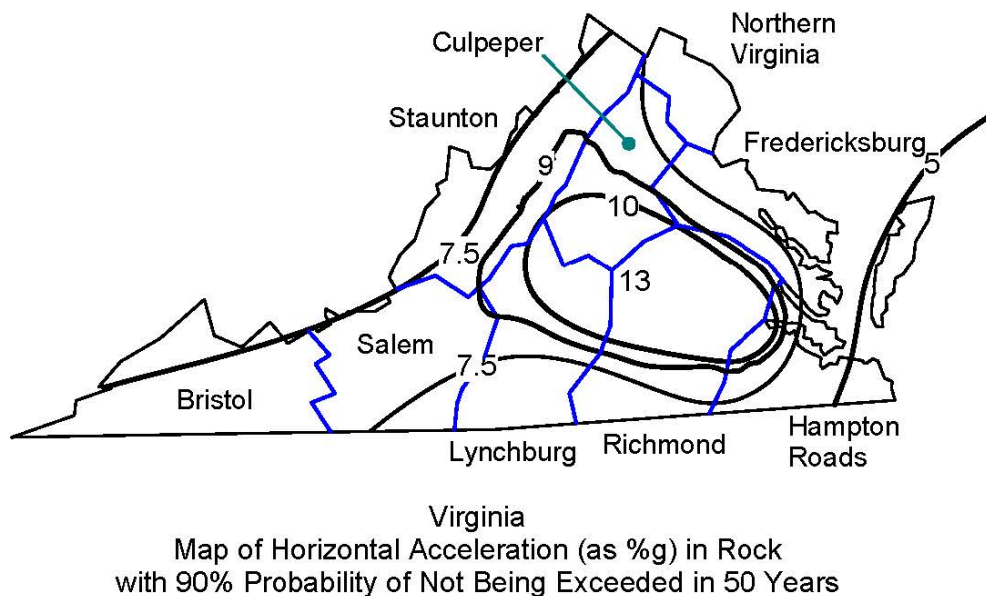


Figure 1. The Peak Ground Acceleration map currently used by the AASHTO Specification. Accelerations are presented as % of g (acceleration due to gravity). The maximum peak ground acceleration for Virginia is 13%g (AASHTO 1996).

New Design Earthquakes and Performance Objectives

The *Standard Specifications* have one maximum design earthquake and two importance classifications for bridges (essential bridges and other bridges). The importance classification is used together with the acceleration coefficient to determine the Seismic Performance Category (SPC) for a given bridge. This is executed differently in the *LRFD Guidelines*, as shown in Table 1.

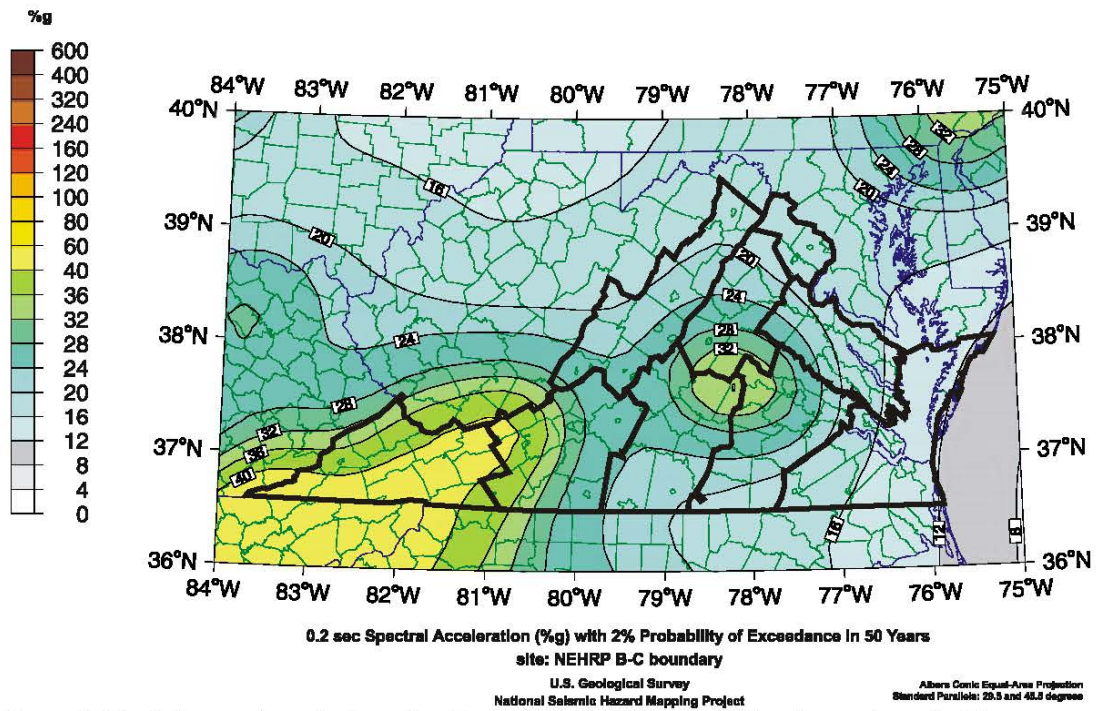


Figure 2. The 0.2-second spectral acceleration map with 2% probability of exceedance in 50 years (USGS 2002)

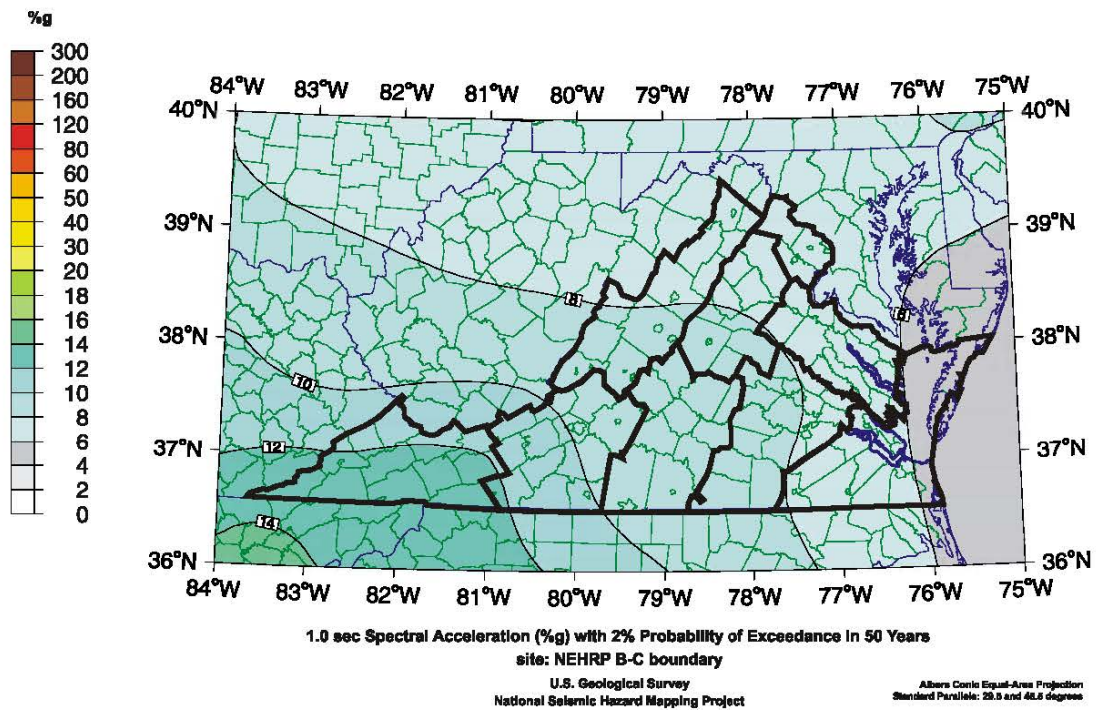
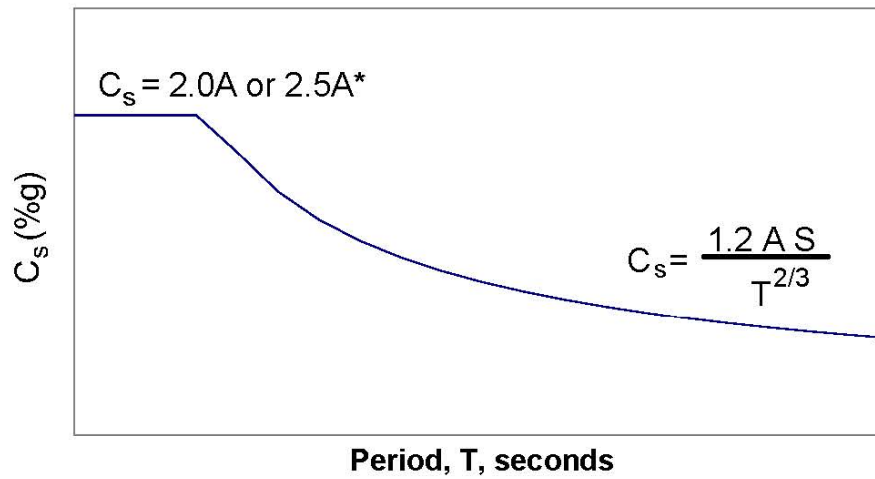


Figure 3. The 1.0-second spectral acceleration map with 2% probability of exceedance in 50 years (USGS 2002).

Elastic Seismic Response Coefficient



*Depends on the soil profile type and A (acceleration coefficient from Figure 1)

Figure 4. The response spectrum curve in *Standard Specifications* (AASHTO 1996).

Design Response Spectrum

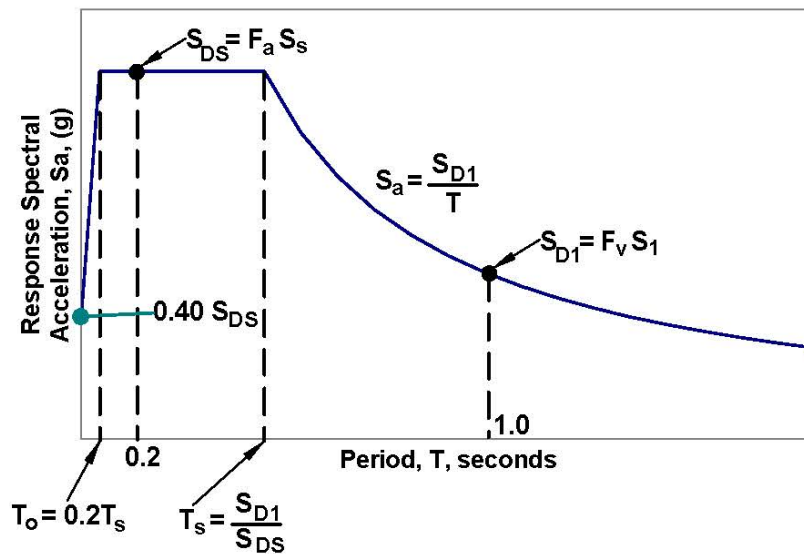


Figure 5. The response spectrum curve in the *LRFD Guidelines* (MCEER 2001).

Table 1. New Design Earthquakes and Performance Objectives in the *LRFD Guidelines* (MCEER 2001).

Probability of Exceedance For Design Earthquake Ground Motions		Performance Level	
		Life Safety	Operational
Maximum Considered Earthquake (MCE) 3% PE in 75 years	Service	Significant Disruption	Immediate
	Damage	Significant	Minimal
Expected Earthquake 50% PE in 75 years	Service	Immediate	Immediate
	Damage	Minimal	Minimal to None

The *LRFD Guidelines* have two design earthquakes: the expected earthquake with a probability of exceedance of 50% in 75 years, and the maximum considered earthquake with a probability of exceedance of 3% in 75 years. In combination with each of these earthquake events, the designer also has to select a performance objective, which determines the acceptable level of service and level of damage for a bridge that has been subjected to a design earthquake.

The two levels are “Life Safety” and “Operational”. For the expected earthquake, all bridges classified in both performance levels are expected to return to immediate service and suffer only minimal damage. For the maximum considered earthquake, the “Life Safety” level bridges are expected to undergo significant service disruptions, such as partial or complete closure of the bridge, and significant structural damage. The “Operational” level bridges are expected to return to immediate service and suffer only minimal damage.

New Soil Factors

The *Standard Specifications* have four soil classifications, and each classification corresponds to a soil factor, which is then used to determine the seismic response coefficients. The *LRFD Guidelines* have six soil classifications, which are used with the spectral acceleration, design earthquake and performance objective to determine the allowable seismic design and analysis procedure (SDAP) and the seismic design requirements (SDR).

New Seismic Design and Analysis Procedures

The *Standard Specifications* have five different seismic design and analysis procedures, which depend on the seismic performance category. These seismic analysis procedures vary from no analysis required to a simple single degree of freedom system analysis to a more complex multi-degree of freedom analysis to a time history analysis. The *LRFD Guidelines* have six seismic design and analysis procedures and six seismic design requirements. One of the two new methods is the Capacity Spectrum Design Procedure, which is a relatively simple procedure that falls between the “no-analysis” method and the “uniform load” method effort wise. It is recommended for very regular structures in low seismic risk regions. The other new method is an elastic response spectrum analysis plus a displacement capacity verification. After the displacement capacity verification is executed, the member forces produced in the elastic response analysis can be reduced by a larger Base Response Modification (R) factor, which then can produce more cost-effective designs.

Primary Changes for Virginia

Spectral Acceleration

Figures 6 and 7 illustrate a comparison between the design response spectrum curves of the *Standard Specifications* and the *LRFD Guidelines* for the Richmond and Bristol areas, respectively. It is important to note that the design response spectrum curves of the *Standard Specifications* were constructed by using the peak ground acceleration map, which had a probability of exceedance of 10% in 50 years, while the design response spectrum curves of the *LRFD Guidelines* were drawn by using the 0.2-second and 1-second period spectral acceleration maps, which had a probability of exceedance of 2% in 50 years. These two different probabilities of exceedance are not equivalent, because they have significantly different return periods. Return period is the average frequency of an exceedance of the peak ground accelerations or spectral accelerations given on the corresponding maps. The formula to compute the return period is given by equation 1:

$$RP = \frac{-T}{\ln(1-P)} \quad (1)$$

RP = return period (years)

T = the number of years of the probability of exceedance

P = the probability of exceedance (number, not percentage)

For a probability of exceedance of 10% in 50 years, the return period is

$$RP = \frac{-50}{\ln(1-0.10)} = 475 \text{ years}$$

For a probability of exceedance of 2% in 50 years, the return period is

$$RP = \frac{-50}{\ln(1-0.02)} = 2475 \text{ years}$$

(Charney 2001)

The difference in the probabilities of exceedance between the maps means that Figures 6 and 7 could only be used to compare the shapes of the design response spectrum curves of the *Standard Specifications* and those of the *LRFD Guidelines*, but not to compare the magnitudes of the spectral accelerations. However, they can be used to compare the magnitude of the equivalent static earthquake forces applied to the structure, which are determined based on the seismic coefficient (S_a or C_s) times the weight of the structure. In some areas of the state, such as the Richmond area, the design seismic forces will be smaller. In other areas, particularly the far southwestern portions, the design seismic forces will be much larger. Although some areas will have lower design seismic forces, the more stringent detailing requirements in the *LRFD Guidelines* could still impact substructure designs.

Comparison of Seismic Response Coefficients for Richmond

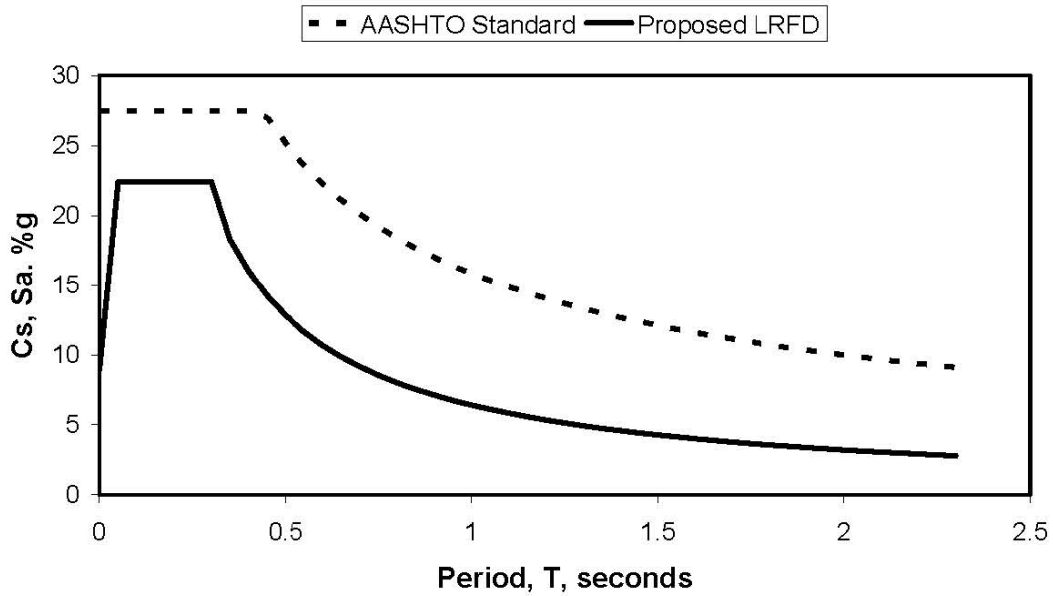


Figure 6. Comparison between the response spectrum curves using the *Standard Specifications* and the *LRFD Guidelines* for the Richmond area (assuming a soil class B).

Comparison of Seismic Response Coefficients for Bristol

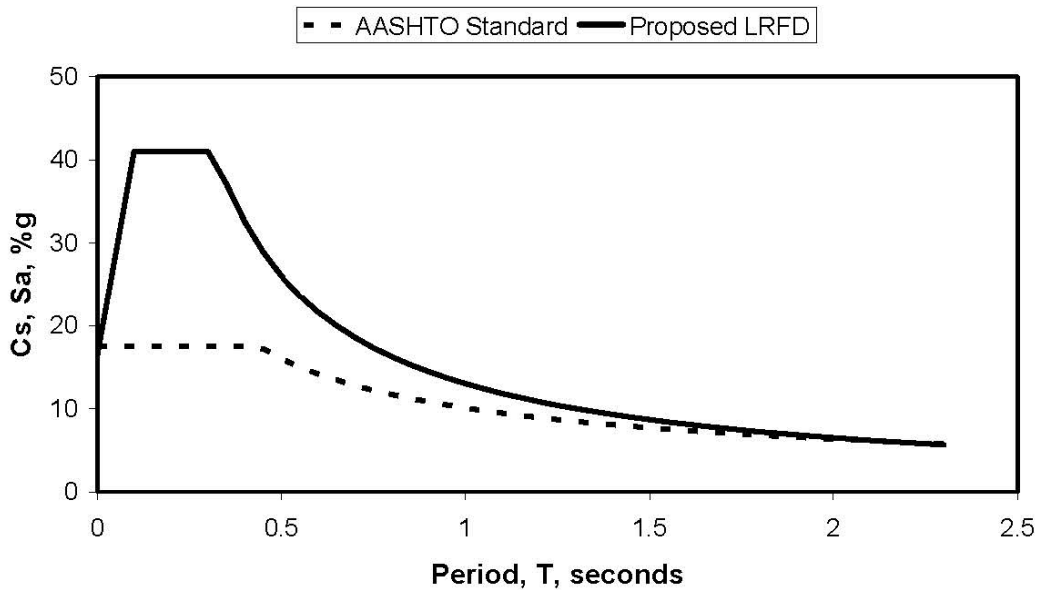


Figure 7. Comparison between the response spectrum curves using the *Standard Specifications* and the *LRFD Guidelines* for the Bristol area (assuming soil class B).

Summary of Changes

It is apparent that the new seismic guidelines represent many changes for Virginia. The level of design effort will be increased in areas newly designated as relatively high seismic risk.

It is also possible that some aspects of typical bridge designs will require modifications to meet the new seismic design requirements as indicated by the increased level of spiral reinforcement required in Richmond despite lower seismic forces shown in the following section. The following sections present the results of the analysis of two typical bridges to evaluate the types of detailing changes that can be expected.

The Prestressed Concrete Girder Bridge

Introduction

This section presents the analysis of a prestressed concrete girder bridge, which is located in Midlothian, a southern suburb of Richmond, Virginia. This bridge was analyzed to investigate if it could endure the maximum considered earthquake, which has a 3% probability of exceedance in 75 years. This bridge was also analyzed to examine if it would satisfy the operational performance level. The maximum considered earthquake and the operational performance level were chosen to ensure that the bridge was held to the highest standard, which means it would perform well during the worst possible earthquake and be operational immediately after the earthquake.

The structure was modeled in RISA 3D to determine the fundamental period of vibration. Then based on the spectral accelerations for the Richmond area, the equivalent seismic loads were determined. These loads were applied to the RISA model to determine earthquake elastic force effects in the structure. After applying the appropriate R factors, the seismic force effects were combined with the dead and live load force effects. Finally the structure was evaluated for compliance with the appropriate seismic design Requirement.

Bridge Configuration

This bridge is a two-span overpass structure, with each span having a length of 124 ft-4 in. The superstructure comprises ten BT72 prestressed concrete beams spaced at 8 ft-6 in center-to-center. The beams support an 8 in deep slab. The slab has a crown at the centerline of the roadway and falls away from center at a 2% cross-slope. The bridge has a 6 ft-5 in wide sidewalk and an aluminum railing on each side. The beams are made continuous with a cast-in-place diaphragm over the center pier, and are cast 7 in into the backwall at each abutment. The bent has five columns, each 3 ft-6 in in diameter, 17 ft-10 in tall, and supported on a 13 ft by 13 ft by 3 ft-6 in deep spread footing. The pier cap is of variable depth, from 5 ft-6 in at each end to 6 ft-2 in at the center. The cap is 4 ft-2 in wide and 80 ft-8.5 in long.

Material Properties

The properties of the materials used in the bridge model are presented in Table 2. It is important to note that two kinds of concrete were used in the bridge model. The prestressed concrete girders have a specified $f_c' = 8000$ psi, while the pier cap beam and columns have $f_c' = 3600$ psi as specified in the construction drawings [VDOT, 2002]. The superstructure slab has a specified $f_c' = 4350$ psi, but it is transformed into the concrete used for the prestressed concrete girder in the section properties calculation. This was required because the superstructure, which consists of the slab and the prestressed concrete girders, is modeled as one member.

The RISA 3D bridge model also used a link to connect the superstructure and the pier cap beam. This link was created to account for the fact that the superstructure rests on the pier cap beam, and therefore the centroid of the superstructure is above that of the pier cap beam. The link was made rigid so that it would not influence the displacements of the members that it connected. Therefore steel material properties were used for the link along with a very large area and moment of inertia to reflect its rigidity, however the density of the link was set to zero, so that it would not impose any unrealistic load on the pier cap beam and columns.

Table 2. Material Properties Used in RISA 3-D Model

Element	Strength, ksi	Modulus of Elasticity, ksi	Shear Modulus, ksi	Poissons Ratio	Unit Weight, pcf
Superstructure	8.0	5100	2200	0.15	150
Substructure	3.6	3400	1480	0.15	150
Rigid Link	60	29,000	10900	0.32	0

Section Properties

To simplify the section properties calculation the deck cross slope was ignored and the superstructure cross section was assumed to look like that shown in Figure 8. In calculating the section properties for the superstructure, the slab properties were transformed into the prestressed concrete girder properties because of the difference in the f_c' values of the slab and the prestressed concrete girders. The complete calculation is provided in Widjaja (2003). The calculated section properties of the superstructure are as follows:

$$\begin{aligned}A &= 13423 \text{ in}^2 \\cg &= 53.1 \text{ in above bottom of girders} \\I_{xx} &= 10.74 \times 10^6 \text{ in}^4 \\I_{yy} &= 11.27 \times 10^8 \text{ in}^4\end{aligned}$$

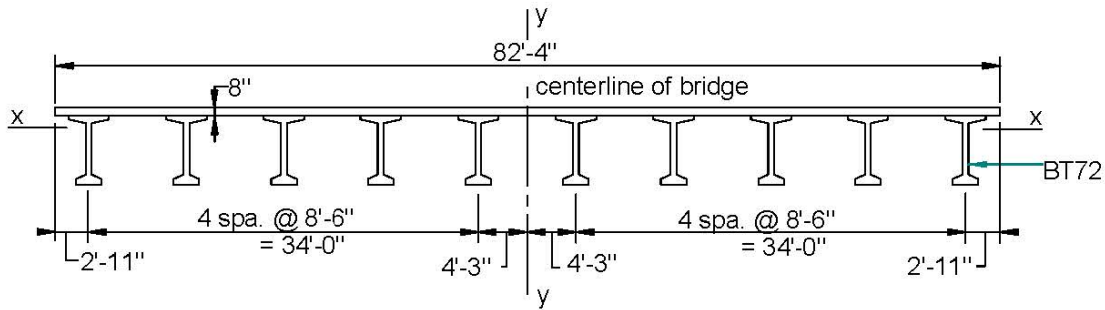


Figure 8. Simplified Cross-Section of Bridge Superstructure.

The simplified center bent used in the analysis is illustrated in Figure 9. The actual pier cap beam does not have a constant cross section due to the 2% cross slope of the top surface. However, for the purpose of calculating the section properties, the average pier cap beam height was used. As mentioned previously, the cap is 4 ft-2 in wide.

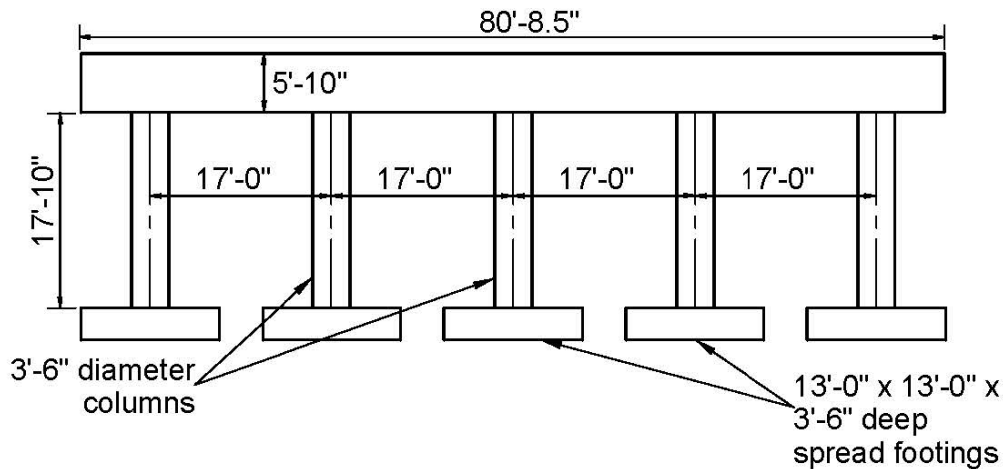


Figure 9. Pier elevation.

Soil Site Class

After the section properties were calculated, the next step was to determine the site class of the soil underneath the bridge, which would be used subsequently to determine the appropriate type of support at the bottom of the column. The classification of the soil under the bridge had to be determined using the site class definitions in the *LRFD Guidelines*. The classification depends on the shear wave velocity (\bar{v}_s), blow count (\bar{N}), or undrained shear strength (\bar{s}_u) in the upper 100 ft of the site profile. The site class definitions in the *LRFD Guidelines* are as follows:

- A Hard Rock with measured shear wave velocity, $\overline{v_s} > 5000$ ft/sec
 - B Rock with $2500 \text{ ft/sec} < \overline{v_s} \leq 5000$ ft/sec
 - C Very dense soil and soft rock with $1200 \text{ ft/sec} < \overline{v_s} \leq 2500$ ft/sec or with either $\overline{N} > 50$ blows/ft or $\overline{s_u} > 2000$ psf
 - D Stiff soil with $600 \text{ ft/sec} \leq \overline{v_s} \leq 1200$ ft/sec or with either $15 \leq \overline{N} \leq 50$ blows/ft or $1000 \text{ psf} \leq \overline{s_u} \leq 2000$ psf
 - E A soil profile with $\overline{v_s} < 600$ ft/sec or with either $\overline{N} < 15$ blows/ft or $\overline{s_u} < 1000$ psf, or any profile with more than 10 ft of soft clay defined as soil with $PI > 20$, $w \geq 40\%$, and $\overline{s_u} < 500$ psf
 - F Soils requiring site-specific evaluations:
 1. Peats and/or highly organic clays ($H > 10$ ft of peat and/or highly organic clay where H = thickness of soil)
 2. Very high plasticity clays ($H > 25$ ft with $PI > 75$)
 3. Very thick soft/medium stiff clays ($H > 120$ ft)
- (MCEER 2001).

After analyzing the boring results, the soil underneath this bridge was classified as class B (Dove 2002).

RISA 3D Model of the Bridge

Once the soil site class underneath the bridge was classified, the bridge RISA 3D model could be drawn. The RISA 3D model of the bridge is shown in Figure 10. As mentioned earlier, a rigid link was used to connect the superstructure and the pier cap beam. The end supports of the superstructure were modeled as springs longitudinally and transversely, and as a pin vertically. It was assumed the beams were free to rotate in all directions because the embedment of the beams into the backwall was relatively short (7 in). This relatively short embedment length was assumed to not fix the beam ends against rotation. The abutment comprises a cap on thirteen H-piles and a backwall that is separated from the cap by a compressible material. It is also interesting that the cap rests on fill that is part of a mechanically stabilized earth header. There is very little information on modeling the stiffness of this type of abutment, so recommendations from Priestly et al.(1996) were adopted. In the longitudinal direction, a stiffness of 200 k/in per foot length of the backwall was used. In the transverse direction, the same soil stiffness was used times the width of the backwall, plus 40 k/in for each pile. This is an area of uncertainty, which would benefit from further research.

The bridge was modeled continuously at the midpoint of the superstructure, where the two spans met, because a continuity diaphragm was shown connecting the girders over the center pier, and the deck was to be cast continuously, with no joint over the center pier.

The site class of the soil underneath the bridge was determined earlier to be class B, and spread footings were used for the foundation of this bridge. Therefore according to Table 3 of this report, which was taken from Table 5.3.4-1 of the *LRFD Guidelines*, the support at the bottom of the columns could be considered to be rigid (fixed). The Foundation Modeling Method (FMM) required for this bridge is FMML.

The joint coordinates of the bridge model were calculated according to the locations of the column center lines, pier cap beam centroidal axis and superstructure centroidal axis. The joint coordinates of the bridge are provided in Appendix I.

Table 3. Definition of Foundation Modeling Method (MCEER 2001).

Foundation Type	FMM I	FMM II
Spread Footing	Rigid	Rigid for Soil Types A and B. For other soil types, foundation springs required if footing flexibility contributes more than 20% to pier displacement
Pile Footing with Pile Cap	Rigid	Foundation springs required if footing flexibility contributes more than 20% to pier displacement
Pile Bent/Drilled Shaft	Estimated depth to fixity	Estimated depth to fixity or soil-springs based on P-y curves.

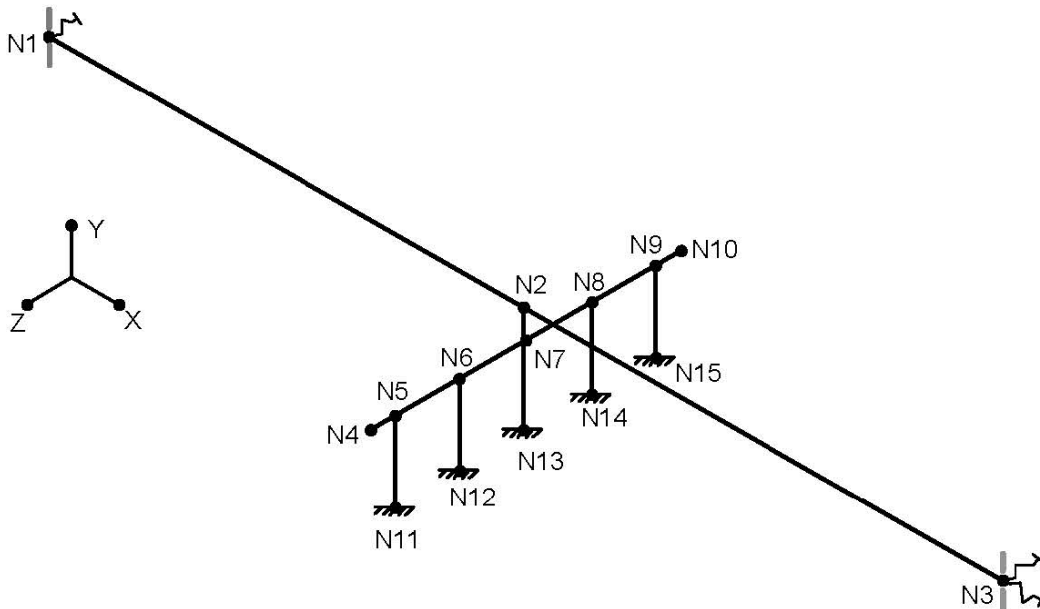


Figure 10. The RISA 3D model of the bridge.

Dead Load Effects

The dead load effects on the pier cap beam and columns were obtained by first applying the self-weight of the superstructure plus a 14 psf allowance for construction tolerances and construction methods as uniformly distributed loads on the superstructure (VDOT 2002). The 14

psf allowance was applied as a uniformly distributed load by multiplying it by the width of the superstructure, which is 82 ft-4 in. The model shown in Figure 10 does not produce accurate dead load effects on the pier cap beam and the columns, because the rigid link connects the midpoint of the superstructure to the middle column, and therefore it produces erroneously high axial loads on the middle column and erroneously low axial loads on the leftmost and rightmost columns. So to more accurately model the transmission of the loads from the superstructure to the substructure, the axial load on the rigid link due to the self-weight of the superstructure and the 14 psf allowance was divided by 10, which was the number of prestressed concrete girders. Then an analysis was performed on the pier structure, in which the pier was subjected to ten point loads on the pier cap beam, each representing a girder.

Live Load Effects

The live load effects were found by adding the maximum effects from the three moving live load cases to the lane load effects. The three moving live load cases and the lane load are shown in Figure 11. The lane load is a 640 lb/ft distributed load (Barker and Puckett 1997). The case that always controlled was the third, which was the two-truck case. Each of these moving live load cases was run along the superstructure, and the largest axial load produced on the rigid link was used to run an analysis on the pier similar to that for the dead loads. The same procedure was also used to determine the lane load effects.

The maximum effects of the three moving load cases, which was always the two-truck case for this bridge, were combined with the lane load effects by using the multiple presence factors (m), the dynamic load allowance (IM), and the 0.9 factor from Section 3.6.1.3.1 of the *AASHTO LRFD Bridge Design Specifications* (AASHTO 1998), since the controlling case was always the two-truck case (Barker and Puckett 1997). The multiple presence factors and the dynamic load allowances are shown in Table 4 and Table 5, respectively.

Since this bridge has four lanes, $m = 0.65$. And since deck joints and fatigue were not the subject of interest in this analysis, $IM = 0.33$. Thus the formula to calculate the live load effects on this bridge was:

$$LL = 0.65 \times 4 \times (1.33 \times 0.9 \times TT + 0.9 \times LN) \quad (2)$$

TT = two-truck load effects
LN = lane load effects

Table 4. The Multiple Presence Factors

Number of Design Lanes	Multiple Presence Factors (m)
1	1.20
2	1.00
3	0.85
More than 3	0.65

Table 5. The Dynamic Load Allowance

Component	Limit State	IM (%)
Deck joints	All	75
All Other Components	Fatigue Fracture	15
	All Other	33

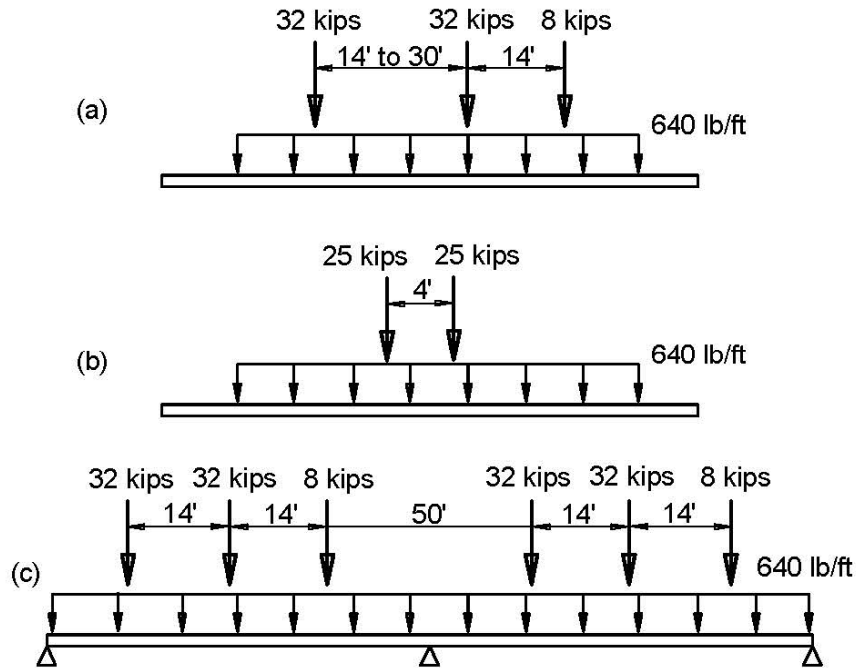


Figure 11. The three moving live load cases and the lane load.

Combined Dead and Live Load Effects on the Columns

The dead and live load effects were combined with the load factors from Table 3.5-1 of the *LRFD Guidelines*. The table presents five strength limit state load combinations, three service limit state combinations, one combination for fatigue and two for extreme events. Since earthquake loading was the focus of this study, the Extreme Event-I combination was chosen, and is as follows:

$$\begin{aligned}
 U = & 1.00 (DC + DD + DW + EH + EV + ES + EL) + \\
 & \gamma_{EQ} (LL + IM + CE + BR + PL + LS) + 1.00(WA) + \\
 & 1.00 (FR) + 1.00 (EQ)
 \end{aligned}
 \tag{3}$$

where: DC = Dead load of structural components and attachments

DD = Downdrag

DW = Dead load of wearing surface and utilities

EH = horizontal earth pressure

EV = vertical pressure from dead load of earth fill

ES = earth surcharge load

EL = accumulated locked in force effects from construction process

LL = vehicular live load

IM = vehicular dynamic load allowance

CE = vehicular centrifugal force

BR = vehicular braking force
 PL = pedestrian live load
 LS = live load surcharge
 WA = water load and stream pressure
 FR = friction
 EQ = earthquake

Suggested values for γ_{EQ} are 0.0, 0.5 and 1.0 (Barker and Puckett 1997). $\gamma_{EQ} = 0.5$ was chosen, which assumes there will not be excessive traffic on the bridge when an earthquake occurs. Thus the combined effects of the dead load and live load are:

$P = DL + (0.5 \times LL)$
 P = combined dead load and live load effects
 DL = dead load effects
 LL = live load effects

The complete results of the dead load and live load effects are presented in Appendix I.

Determination of the Required Seismic Design and Analysis Procedure (SDAP) and Seismic Design Requirement (SDR)

In order to determine the required Seismic Design and Analysis Procedure (SDAP) and Seismic Design Requirement (SDR) for this bridge, first the following parameters must be determined:

S_s = 0.2-second period spectral acceleration, obtained from the USGS website zip code lookup for spectral accelerations at the location of the bridge
 S_1 = 1-second period spectral acceleration, obtained from the USGS website zip code lookup for spectral accelerations at the location of the bridge
 F_a = site coefficients for the short-period range, which are given in Table 6
 F_v = site coefficients for the long-period range, which are given in Table 7

The 0.2-second and 1-second period spectral acceleration maps are based on a probability of exceedance of 2% in 50 years, but all the analyses in this study were performed to investigate if the bridges could endure a maximum considered earthquake, which has a probability of exceedance of 3% in 75 years. The return periods for both probabilities of exceedance were computed to prove that they are approximately equivalent.

For the probability of exceedance of 2% in 50 years, the return period is:

$$RP = \frac{-50}{\ln(1 - 0.02)} = 2475 \text{ years} \quad (1)$$

For the probability of exceedance of 3% in 75 years, the return period is:

$$RP = \frac{-75}{\ln(1 - 0.03)} = 2462 \text{ years} \quad (1)$$

(Charney, 2001).

Since the return periods for the two different probabilities of exceedance are close, using the spectral acceleration maps which were based on a probability of exceedance of 2% in 50 years to analyze this bridge for the maximum considered earthquake with a probability of exceedance of 3% in 75 years was proved acceptable.

Table 6. Values of F_a as a Function of Site Class and Mapped Short-Period Spectral Acceleration (MCEER 2001).

Site Class	Mapped Spectral Response Acceleration at Short Periods				
	$S_s \leq 0.25$ g	$S_s = 0.50$ g	$S_s = 0.75$ g	$S_s = 1.00$ g	$S_s \geq 1.25$ g
A	0.8	0.8	0.8	0.8	0.8
B	1.0	1.0	1.0	1.0	1.0
C	1.2	1.2	1.1	1.0	1.0
D	1.6	1.4	1.2	1.1	1.0
E	2.5	1.7	1.2	0.9	0.9
F	a	a	a	a	a

Note: a -Site-specific geotechnical investigation and dynamic site response analyses must be performed.

Table 7. Values of F_v as a Function of Site Class and Mapped 1.0 Second Period Spectral Acceleration (MCEER 2001).

Site Class	Mapped Spectral Response Acceleration at 1 Second Periods				
	$S_1 \leq 0.1$ g	$S_1 = 0.2$ g	$S_1 = 0.3$ g	$S_1 = 0.4$ g	$S_1 \geq 0.5$ g
A	0.8	0.8	0.8	0.8	0.8
B	1.0	1.0	1.0	1.0	1.0
C	1.7	1.6	1.5	1.4	1.3
D	2.4	2.0	1.8	1.6	1.5
E	3.5	3.2	2.8	2.4	2.4
F	a	a	a	a	a

Note: a- Site-specific geotechnical investigation and dynamic site response analyses must be performed.

This bridge is located in Midlothian, a southern suburb of Richmond. The zip code for Midlothian is 23113, which was input into the USGS website zip code lookup for spectral accelerations. For this bridge, the following values were obtained:

$$S_s = 0.287 \text{ g}$$

$$S_1 = 0.0833 \text{ g}$$

(USGS 2002b)

Since the soil is class B, $F_a = 1.0$ and $F_v = 1.0$, therefore:

$$S_{DS} = F_a S_s = (1.0)(0.287 \text{ g}) = 0.287 \text{ g}$$

$$S_{D1} = F_v S_1 = (1.0)(0.0833 \text{ g}) = 0.0833 \text{ g}$$

The values of $F_v S_1$ and $F_a S_s$ were used to determine the Seismic Hazard Level according to Table 8 of this report, which was taken from Table 3.7-1 of the *LRFD Guidelines*. When two different Seismic Hazard Levels are required by the values of $F_v S_1$ and $F_a S_s$, the higher level controls. Therefore Seismic Hazard Level II was assigned to this bridge.

Table 8. Seismic Hazard Levels (MCEER 2001).

Seismic Hazard Level	Value of $F_v S_1$	Value of $F_a S_s$
I	$F_v S_1 \leq 0.15$	$F_a S_s \leq 0.15$
II	$0.15 < F_v S_1 \leq 0.25$	$0.15 < F_a S_s \leq 0.35$
III	$0.25 < F_v S_1 \leq 0.40$	$0.35 < F_a S_s \leq 0.60$
IV	$0.40 < F_v S_1$	$0.60 < F_a S_s$

The Seismic Hazard Level was used to determine the required Seismic Design and Analysis Procedure (SDAP) and Seismic Design Requirement (SDR) by using Table 9 of this report, which was taken from Table 3.7-2 of the *LRFD Guidelines*.

Table 9. Seismic Design and Analysis Procedures (SDAP) and Seismic Design Requirements (SDR) (MCEER 2001).

Seismic Hazard Level	Life Safety		Operational	
	SDAP	SDR	SDAP	SDR
I	A1	1	A2	2
II	A2	2	C/D/E	3
III	B/C/D/E	3	C/D/E	5
IV	C/D/E	4	C/D/E	6

Since Seismic Hazard Level II was assigned to this bridge and the operational performance objective was chosen, SDAP C, D or E would be required for this bridge. But according to Section 4.4.2 of the *LRFD Guidelines*, SDAP C could not be used for this bridge because this bridge had fewer than three spans. Thus SDAP D was required for this bridge. The required Seismic Design Requirement (SDR) for this bridge was SDR 3 according to Table 9 of this report. In the next step, the cracked section properties of the columns and pier cap beam are determined because SDAP D uses an elastic (cracked section properties) analysis. If the bridge were analyzed for the Expected Earthquake and the Life Safety performance level, this bridge would require no additional analysis, and the Seismic Design Requirement would be SDR 2.

Cracked Section Properties of the Columns

The combined axial loads from the dead and live loads were used to obtain the cracked section properties of the columns, i.e. the effective moment of inertia about the x-axis (I_{exx}) and the effective moment of inertia about the y-axis (I_{eyy}). The relationship between the gross cross-sectional properties and the effective cross-sectional properties that should be used in analysis is dependent on the magnitude of the axial load and the reinforcement ratio in the column. Higher axial loads result in less cracking and hence a larger percentage of the gross properties can be assumed effective. Similarly, a larger reinforcement ratio will result in larger effective section properties. For this analysis recommendations by Priestley et al.(1996) were used. The relationship between the total axial load on the column, the reinforcement ratio, and the effective moment of inertia (I_e) is shown in Figure 12.

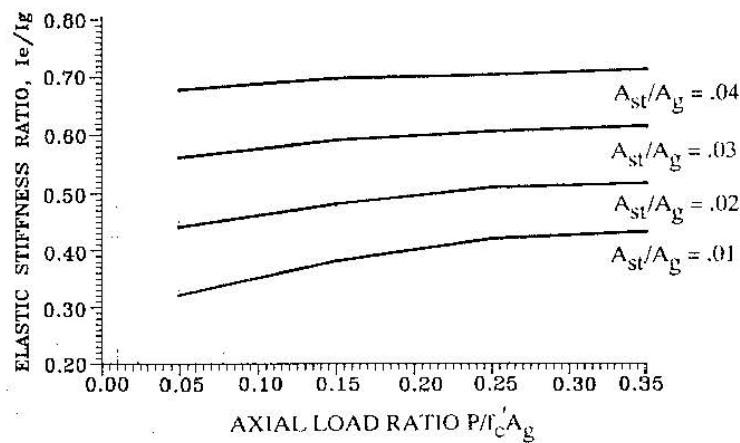
For this bridge the columns were 3 ft-6 in in diameter and contained 18 each No. 11 reinforcing bars. Their reinforcement ratio is:

$$\frac{A_{st}}{A_g} = \frac{18 \cdot 1.56 \text{in}^2}{(42 \text{in})^2 \cdot \frac{\pi}{4}} = 0.02 \quad (4)$$

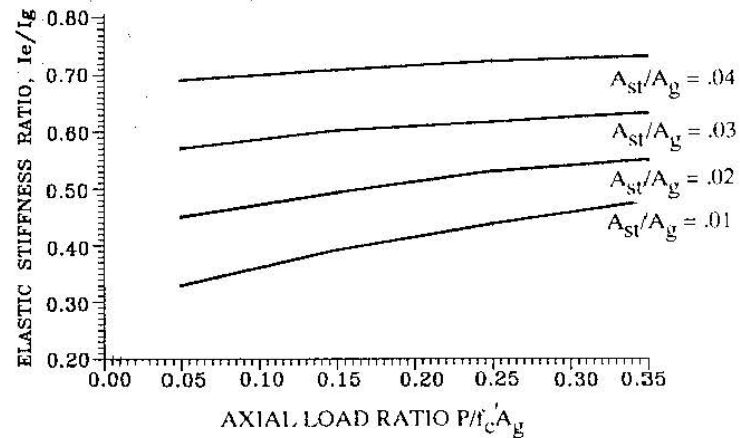
And from Appendix I:

$$\frac{P_{avg}}{f'_c \cdot A_g} = \frac{805 \text{kips}}{3.6 \text{ksi} \cdot 1385 \text{in}^2} = 0.162 \quad (5)$$

Thus, with a known reinforcement ratio A_{st}/A_g , and known $P/f'_c A_g$ the effective moment of inertia I_e can be determined. For this bridge, I_e/I_g was approximately 0.49. The spreadsheet for this calculation is also presented in Appendix I.



a) Circular Sections



b) Rectangular Sections

Figure 12. The relationship between axial load on the column, reinforcement ratio and effective moment of inertia I_e (Priestley et al 1996).

Cracked Section Properties of the Pier Cap Beam

The cracked section properties of the pier cap beam, i.e. I_{exx} and I_{eyy} , can be obtained by using either of two methods: the moment-curvature method (Priestley et al. 1996) and the method presented in the ACI 318-02 Building Code (ACI 2002). The moment-curvature relationship uses the following equation:

$$EI_e = \frac{M_y}{\phi_y} \quad (6)$$

M_y = the yield moment in the moment-curvature relationship for the cross section

ϕ_y = the yield curvature in the moment-curvature relationship for the cross section

The cracked section properties using this method produced $I_e = 0.17 I_g$. The complete calculation for this method is presented in Widjaja (2003).

Using the ACI method revealed that the pier cap beam was not expected to be cracked at service load level, since $M_{cr} > M_a$ (the maximum positive or negative moment in the pier cap beam) and therefore $I_e = I_g$.

Despite the discrepancy between the results of the moment-curvature method and the ACI method, the moment-curvature result was used. It was assumed that in the presence of earthquake forces, or other unforeseen effects such as differential settlement, the cap would be cracked.

Section Properties of the Superstructure

The superstructure's gross section properties were used for the analysis of the bridge. After completion of the analysis, the assumption was checked by comparing the maximum moment in the superstructure to the cracking moment. The assumption of uncracked properties was proven to be correct. This calculation is presented in Widjaja (2003).

Period of Vibration

After obtaining the cracked section properties for the pier cap beam and the columns, the RISA 3D model of the bridge was modified by changing the gross section properties to the cracked section properties. The next step was to compute the period of vibration of the bridge. For comparison, two methods were used to calculate the period of vibration, the uniform load method and the single mode spectral analysis method (MCEER 2001).

Uniform Load Method

The uniform load method is an equivalent static method of analysis that uses a uniform lateral load to approximate the effect of seismic loads. The method is suitable for common bridges that respond primarily in their fundamental mode of vibration.

The first step of this method was to apply a uniformly distributed load p_o , which can be set arbitrarily to any magnitude according to one's preference, over the length of the bridge. For this bridge analysis, p_o was set to 570 lb/in so that the resulting deflections would have a reasonable magnitude. Each span of the bridge was divided into sections, eleven in this case, and the lateral displacement of each section was called $v_s(x)$. The bridge lateral loading is shown in Figure 13.

Based on the output from the RISA analysis, the bridge's lateral stiffness (K) and total weight (W) were calculated by using equations 7 and 8, respectively.

$$K = \frac{P_o L}{v_{s,MAX}} \quad (7)$$

L = total length of the bridge = 248.7 ft
 $v_{s,MAX}$ = maximum value of $v_s(x)$ = 0.76 in
 K = 2,240 kips/in

$$W = \int w(x) dx \quad (8)$$

$w(x)$ = weight per unit length of the dead load of the bridge superstructure and tributary substructure
 W = 6240 kips

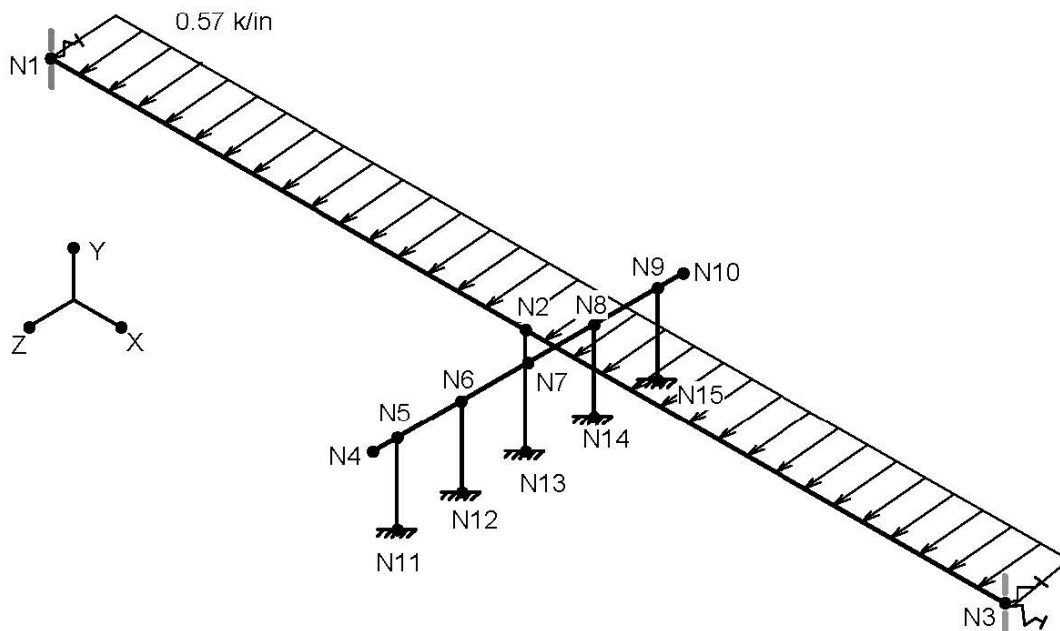


Figure 13. The uniform lateral loading on the bridge.

The fundamental period of vibration was calculated using equation 9:

$$T = 2\pi \sqrt{\frac{W}{gK}} \quad (9)$$

g = acceleration of gravity = 386 in/sec²

T = 0.534 sec.

(MCEER 2001).

The uniform load method was also used to determine the fundamental period of vibration for the bridge in the longitudinal direction with calculations as follows:

$$K = \frac{P_o}{v_{s,MAX}} \quad (7)$$

P_o = arbitrary load applied on superstructure at top of rigid link = 1870 k

v_{s,MAX} = maximum value of v_s(x) = 0.15 in

K = 12,470 kips/in

$$T = 2\pi \sqrt{\frac{W}{gK}} \quad (9)$$

T = 0.226 sec.

Single Mode Spectral Analysis Method

The primary difference between this method and the uniform load method is that the equivalent lateral earthquake forces for this method are not uniformly distributed loads over the length of the bridge. The magnitude varies over the length of the bridge, as a function of the lateral displacement at each point. The complete calculation of the period of vibration using the single mode spectral analysis method is presented in Widjaja (2003).

As in the uniform load method, first the bridge was subjected to a uniform load p_o of 570 lbs/in, and the resulting deflection of each of the eleven sections as given by RISA 3D was called v_s(x). Then the α, β, and γ factors were calculated as follows:

$$\alpha = \int v_s(x) dx \quad (10)$$

$$\beta = \int w(x)v_s(x) dx \quad (11)$$

$$\gamma = \int w(x)v_s(x)^2 dx \quad (12)$$

w(x) = the weight per length of the dead load of the bridge superstructure and tributary substructure.

For this bridge,

$$\alpha = 2173 \text{ in}^2$$

$$\beta = 4682 \text{ kip}\cdot\text{in}$$

$$\gamma = 3416 \text{ kip}\cdot\text{in}^2$$

Then the period of the bridge can be calculated from the expression:

$$T = 2\pi \sqrt{\frac{\gamma}{p_o g \alpha}} \quad (13)$$

T = 0.531 sec. for this bridge.
(MCEER, 2001).

The period of vibration obtained by using the uniform load method was very similar to that obtained using the single mode spectral analysis method. The uniform load method assumes equal participation of all of the mass of the structure, as if all the mass is lumped at the top of the pier. The single mode spectral analysis is more of a weighted average, describing the structure and accounting for the mass and the displacement along the length of the structure. In this case the periods were very similar because of the springs used to model the abutments. The displacements at the abutments were almost as large as those at the center pier (0.69 in compared to 0.76 in), so the entire mass of the superstructure moves almost as a rigid body, which is the assumption in the uniform load method.

Design Response Spectrum Curve

After the period of vibration was determined, the next step was to draw the design response spectrum curve, from which the spectral acceleration (S_a) can be obtained. The general shape of a design response spectrum curve was shown earlier as Figure 5. The required values for the generation of the curve are as follows:

$$\begin{aligned} S_{DI} &= 0.0833 \text{ g} \\ S_{DS} &= 0.287 \text{ g} \\ T_s &= \frac{S_{DI}}{S_{DS}} = \frac{0.0833 \text{ g}}{0.287 \text{ g}} = 0.290 \text{ sec} \end{aligned} \quad (14)$$

$$T_o = 0.2 T_s = 0.2 (0.290 \text{ sec}) = 0.058 \text{ sec} \quad (15)$$

(MCEER 2001).

The design response spectrum curve for this bridge is given in Figure 14. For the three fundamental periods of vibration, the spectral accelerations are as follows:

Uniform load transverse period	T = 0.534 sec	$S_a = 0.156$
Longitudinal period	T = 0.226 sec	$S_a = 0.287$
Single mode spectral transverse	T = 0.531 sec	$S_a = 0.157$

Equivalent Earthquake Forces

After obtaining the spectral acceleration from the design response spectrum curve, the equivalent earthquake forces can be computed. As for the period of vibration, the equivalent

earthquake forces can be computed using either the uniform load method or the single mode spectral analysis method (MCEER 2001).

Uniform Load Method

The equivalent earthquake force, p_e , was calculated using the expression:

$$p_e = \frac{S_a W}{L} \tag{16}$$

S_a = the spectral acceleration from the design response spectrum curve (MCEER 2001).

For this bridge in the transverse direction, $p_e = 3.91$ kip/ft, and in the longitudinal direction, $p_e = 7.2$ kip/ft.

Single Mode Spectral Analysis Method

The equivalent earthquake force computed using this method is not a uniformly distributed load as in the uniform load method. Instead the lateral earthquake load varies with mass and displacement along the length of the structure. The equivalent earthquake force, p_e , is calculated using the expression:

$$p_e(x) = \frac{\beta S_a}{\gamma} w(x) v_s(x) \tag{17}$$

$p_e(x)$ = the equivalent earthquake force for that section (MCEER 2001).

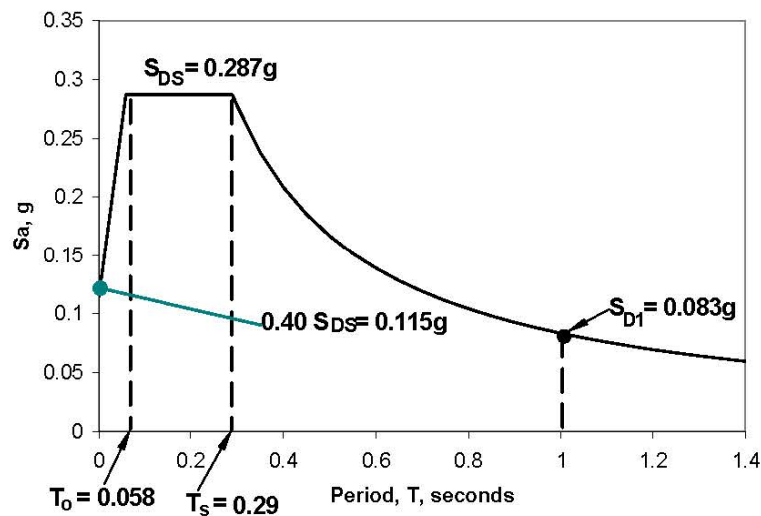


Figure 14. The design response spectrum curve for this bridge.

Each span of the bridge was divided into eleven sections and each section of the span had a different deflection, $v_s(x)$, and mass. As a result, each section had a different equivalent earthquake force. The equivalent earthquake loading for the bridge using this method is shown in Figure 15. The distributed load in the middle is much larger than the other distributed loads, because the distributed load in the middle carries the tributary load of the substructure. The complete calculation to determine the equivalent earthquake force using this method is presented in Widjaja (2003).

Combined Effects of the Dead, Live and Earthquake Loads

The final analysis of the bridge was performed using the cracked section properties for dead, live and earthquake loads. The procedure to calculate the dead and live load effects for this final analysis was the same as that used to perform the analysis to determine the dead and live load effects to obtain cracked section properties. For the earthquake loads, the axial loads, moments and shears for the pier cap beam and columns were taken directly from the analysis on the entire bridge. The load factors used to combine the dead, live and earthquake load effects were given earlier (Extreme Event-I load combination (Equation 3)). But for the earthquake loads, the responses (axial loads, moments and shears) were divided by the R factor given in Table 10.

Since SDAP D (Elastic Response Spectrum Method) and the Operational performance level were used in this research study, according to Table 10 the earthquake load responses on the columns could be divided by $R=1.5$. Thus the combined effects of the dead, live and earthquake loads are given by the following expression:

$$P = 1.0DL + 0.5LL + 1.0\left(\frac{EQ}{1.5}\right) \quad (18)$$

The responses in the two orthogonal directions were combined using the recommendations of the *LRFD Guidelines*. This required examining two possible combinations of earthquake effects: 40% of the longitudinal effect plus 100% of the lateral and 100% of the longitudinal effect plus 40% of the lateral. The vector sum of these two effects plus the dead and live load effects were compared to determine the worst cast combination.

The complete results of the dead, live and earthquake load effects are given in Appendix I.

Column Strength under Flexure and Axial Loads

The interaction diagram of the columns was constructed to determine if the combinations of axial load and moment exceeded the capacity of the column. The complete calculation of the points of the interaction diagram is provided in Widjaja (2003). For all the columns of this bridge, the maximum axial load and moment were extremely low compared to the capacity of the column, as shown in Figure 16.

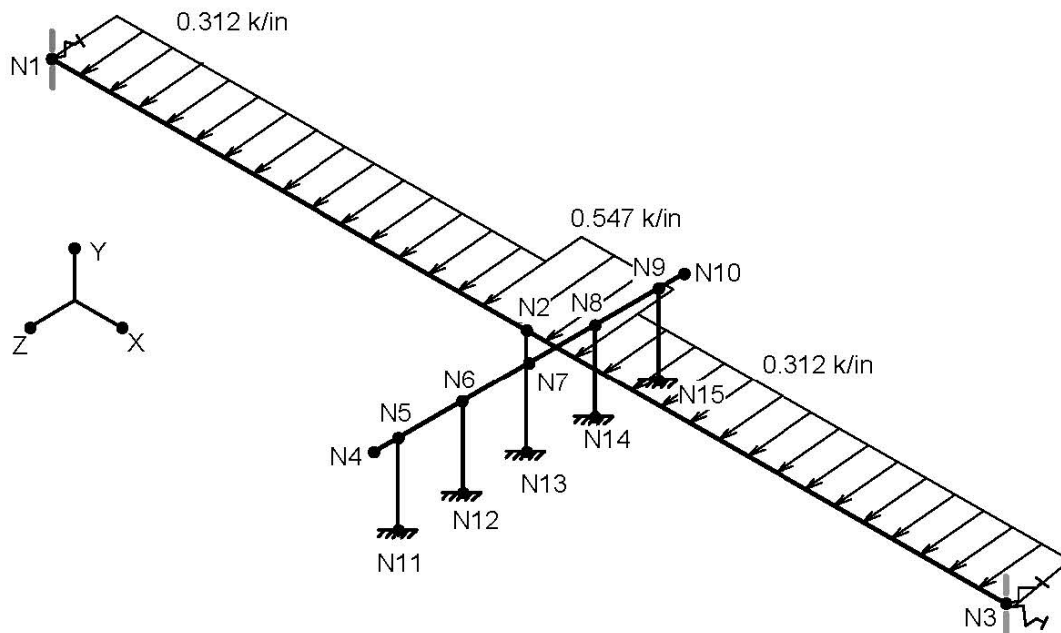


Figure 15. The equivalent earthquake loading using the single mode spectral analysis method.

Table 10. Base Response Modification Factors, R, for Substructure (MCEER 2001).

Substructure Element	Performance Objective			
	Life Safety		Operational	
	SDAP D	SDAP E	SDAP D	SDAP E
Wall Piers – larger dimension	2	3	1	1.5
Columns – single and multiple	4	6	1.5	2.5
Pile bents and drilled shafts – vertical piles – above ground	4	6	1.5	2.5
Pile bents and drilled shafts – vertical piles – 2 diameters below ground level – no owners approval required	1	1.5	1	1
Pile bents and drilled shafts – vertical piles – in ground – owners approval required	N/A	2.5	N/A	1.5
Pile bents with batter piles	N/A	2	N/A	1.5
Seismically isolated structures	1.5	1.5	1	1.5
Steel braced frame – ductile components	3	4.5	1	1.5
Steel braced frame – nominally ductile components	1.5	2	1	1
All elements for expected earthquake	1.3	1.3	0.9	0.9

Flexural Strength of the Pier Cap Beam

The flexural strength of the pier cap beam was calculated and compared to the maximum factored moment in the pier cap beam. In order to simplify the calculation of the flexural strength, the side reinforcing bars of the pier cap beam were ignored. The actual cross section of the pier cap beam, was simplified to that shown in Figure 17. The complete calculation of the flexural strength of the pier cap beam is presented in Widjaja (2003). For the pier cap beam of this bridge,

$$\begin{aligned}\phi M_n &= 2790 \text{ ft-kips} \\ M_u &= 2222 \text{ ft-kips} \\ \phi M_n &> M_u\end{aligned}$$

Thus the flexural capacity of the pier cap beam was not exceeded.

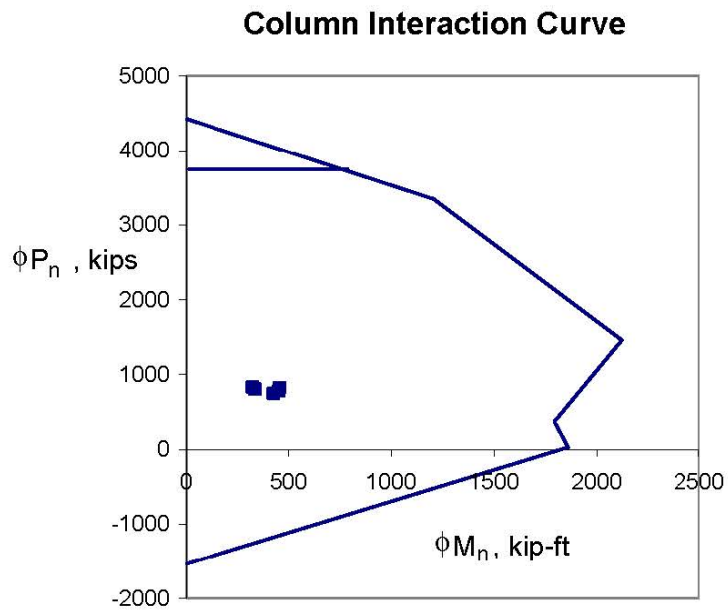


Figure 16. The interaction diagram for the columns of the prestressed concrete girder bridge (42 in diameter column with 18 No. 11 bars). The points are the factored axial loads and moments in the columns.

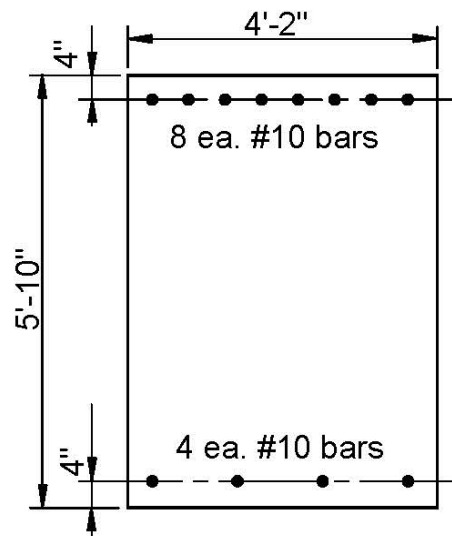


Figure 17. The simplified cross section of the pier cap beam.

Detailing Changes due to the New LRFD Guidelines

The details of the bridge were checked according to the appropriate Seismic Design Requirement, which was SDR 3 for this bridge. The summary of the checks is given in Table 11, with the requirements that were not satisfied shaded. In addition the expected maximum lateral displacement was checked, and found to be quite small at 0.4 in.

The critical detailing checks involved the spiral reinforcement in the columns and in the beam-column and footing-column joints. The reinforcing had to be checked to ensure that it provided adequate confinement to the core, provided adequate shear strength, and provided adequate bracing to prevent the longitudinal bars from buckling.

Using current *Standard Specifications* seismic design provisions and peak ground acceleration maps, the existing design is adequate. The peak ground acceleration is 11.5%. If the bridge is assumed essential, it is classified as Seismic Performance Category B (SPC B). The soil profile of stiff clays less than 30 ft deep over rock is considered soil profile I. With this information and the previously calculated period of vibration of the bridge of 0.534 sec, the response coefficient is:

$$C_s = \frac{1.2AS}{T^{2/3}} = \frac{1.2 \cdot 0.115 \cdot 1.0}{(0.534)^{2/3}} = 0.21$$

This is higher than the coefficient calculated with the new *LRFD Guidelines*. However, it should be noted that the R value for multi-column bents in the *Standard Specification* is 5 as compared to 1.5 in the *LRFD Guidelines*. Also differences in load combinations and live loads between the two methods could result in slightly different column stiffnesses used in the analysis. The detailing requirements are not as stringent in the *Standard Specification*, so even though the new guidelines result in smaller seismic forces, the bridge design must be altered to adhere to new detailing requirements.

To bring this bridge up to the new standards, the spiral spacing must be changed from 5 in to 4 in, and the spiral reinforcing must be carried up through the full height of the cap and down into the footing. This results in an additional 2000 lb of reinforcing steel in the bridge, which will result in an approximately 0.1% increase in the total construction cost. The complete detailing requirements and cost increase calculations are presented in Widjaja (2003).

Table 11. The results of the detailing requirement checks for the bridge using Seismic Design Requirement 3.

Number	Requirement	Required	Provided
1a	Transverse Reinforcement Ratio in Potential Plastic Hinge Zones Using the Implicit Shear Detailing Approach	0.00285	0.00362
1b	Transverse Reinforcement Ratio outside the Plastic Hinge Zones Using the Implicit Shear Detailing Approach	0.00160	0.00362
3	Transverse Reinforcement Ratio for Confinement at Plastic Hinges	0.00687	0.00724
4	Spiral Spacing for Confinement at Plastic Hinges	4 in	5 in
5	Transverse Spiral Reinforcement Ratio at the Moment Resisting Connection between the Column and the Pier Cap Beam using explicit approach	0.003501	0.00724 (if spiral is extended into cap beam)
6	Stirrups in the Pier Cap Beam within half Of the cap depth on either side of the column	4.5 in ²	9.9 in ²

The Steel Girder Bridge

Introduction

This section presents the analysis of a pair of steel girder bridges, West Bound and East Bound, which are located in Tazewell County, 70 miles northeast of Bristol, in the southwestern part of Virginia. They were built at the same time in 1993. These bridges are parallel and adjacent to each other. The West Bound bridge has two lanes, and the East Bound bridge has three lanes (VA DOT 1993). These bridges were analyzed to investigate if they could endure the maximum considered earthquake, which has a 3% probability of exceedance in 75 years. These two bridges were also analyzed to examine if they would satisfy the operational performance level. The maximum considered earthquake and the operational performance level were chosen to ensure that the bridges were held to the highest standard, which means they would perform well during the worst possible earthquake and be operational immediately after the earthquake.

Similarly to the prestressed concrete girder bridge, the bridges were modeled in RISA 3D to determine their fundamental periods of vibration. Then based on the spectral accelerations for the Bristol area, the equivalent seismic loads were determined. These loads were applied to the RISA model to determine earthquake elastic force effects in the structures. After applying the appropriate R factors, the seismic force effects were combined with the dead and live load force effects. Finally the structures were evaluated for compliance with the appropriate Seismic Design Requirement.

Bridge Configuration

The bridges are both two-span overpass structures. The West Bound bridge spans are 99 ft and 96 ft-4 in long, while the East Bound bridge spans are 99 ft-3 in and 96 ft-9 in long. Both bridges have a skew of approximately 37 degrees. The West Bound superstructure comprises five steel plate girders, with 54 in deep webs and variable depth flanges, placed at a 9 ft-4 in

center-to-center spacing. The East Bound superstructure comprises six steel plate girders, with 54 in deep webs and variable depth flanges, placed at a 9 ft-11 in center-to-center spacing. The girders are continuous from abutment to abutment, with two permissible field splices on each girder. The slabs are 8.5 in thick and cast continuously from abutment to abutment with no joints. The center pier of the West Bound bridge has three columns, each 3 ft-6 in in diameter and an average of 18 ft-5.5 in tall, supported on 10 ft-6 in by 10 ft-6 in by 3 ft deep spread footings. The pier cap is 4 ft deep, 3 ft-9 in wide and 54 ft long. The center pier of the East Bound bridge has four columns, each 3 ft-6 in in diameter and an average of 17 ft-4.5 in tall, supported on 10 ft-6 in by 10 ft-6 in by 3 ft deep spread footings. The pier cap is 4 ft deep, 3 ft-9 in wide and 69 ft-6 in long.

Material Properties

The properties of the materials used in the bridge model are presented in Table 12. It is important to note that there are two kinds of concrete used in the bridge model. The superstructure has a specified $f_c' = 4000$ psi, while the pier cap beam and columns have a specified $f_c' = 3000$ psi. There are also two kinds of steel used for the bridge, 50 ksi and 36 ksi. The 50 ksi steel is used for the plate girder webs and flanges, while the 36 ksi steel is used for all other structural steel, including diaphragms, stiffeners, connector plates, and bearings (VDOT 1993). However, the calculation of the section properties of the superstructure, which combines the plate girder and the slab, uses only the 50 ksi steel.

The RISA 3D model of the bridges used a rigid link for each bridge to connect the superstructure and the pier cap beam. This link was created to account for the fact that the superstructure rests on the pier cap beam, and therefore the centroid of the superstructure is above that of the pier cap beam. The link was made rigid so that it would not influence the displacements of the members that it connected. Therefore, steel material properties were used along with a very large area and moment of inertia for the link to reflect its rigidity, however the density of the link was set to zero, so that it would not impose any unrealistic load on the pier cap beam and columns.

Table 12. Material Properties Used in RISA 3-D Model

Element	Strength, ksi	Modulus of Elasticity, ksi	Shear Modulus, ksi	Poissons Ratio	Unit Weight, pcf
Superstructure Concrete	4.0	3610	1570	0.15	150
Substructure Concrete	3.0	3120	1360	0.15	150
Superstructure Steel	50	29,000	11,000	0.32	490
Rigid Link Steel	50	29,000	11,000	0.32	0

Section Properties

To simplify the section properties calculation, the superstructure cross sections are assumed to be those shown in Figures 18 and 19. In calculating the section properties for the superstructure, the slab properties are transformed into the steel girder properties because of the difference in the E values of the concrete slab and the steel girders. The complete section property calculations are presented in Widjaja (2003). The important section properties of the superstructure are as follows:

West Bound:

$$A = 899 \text{ in}^2$$

$$cg = 52.5 \text{ in from bottom}$$

$$I_{xx} = 373,000 \text{ in}^4$$

$$I_{yy} = 25,600,000 \text{ in}^4$$

East Bound:

$$A = 1114 \text{ in}^2$$

$$cg = 51.9 \text{ in from bottom}$$

$$I_{xx} = 521,000 \text{ in}^4$$

$$I_{yy} = 50,500,000 \text{ in}^4$$

The simplified center piers used in the analyses are illustrated in Figures 20 and 21. The three columns of the West Bound pier were modeled as 18 ft-5.5 in tall from top of footing to bottom of cap. However, to accommodate the cross-slope the columns actually had heights of 18 ft- 8.625 in, 18 ft-5.5 in and 18 ft-2.375 in. The four columns of the East Bound pier were modeled as 17 ft-4.5 in, however actual column heights varied from 17 ft-9.125 in to 17 ft-0.125in. As mentioned previously, the caps are 3 ft-9in wide.

Soil Site Class

After the section properties were calculated, the next step was to determine the site class of the soil underneath the bridges. The classification of the soil under the bridges had to be determined using the site class definitions in the *LRFD Guidelines*, which depend on the shear wave velocity (\bar{v}_s), blow count (\bar{N}), or undrained shear strength (\bar{s}_u) in the upper 100 ft of the site profile. The site class definitions in the *LRFD Guidelines* were presented in the previous section. After analyzing the boring results, the soil underneath the two bridges was classified as class B (Dove, 2002).

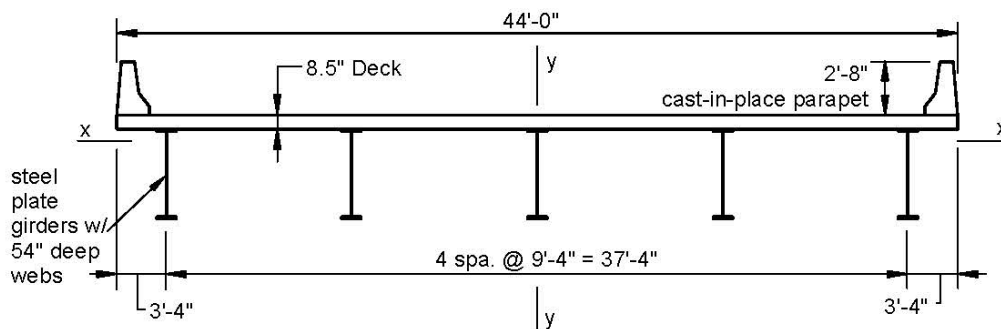


Figure 18. The simplified cross section of the West Bound bridge superstructure.

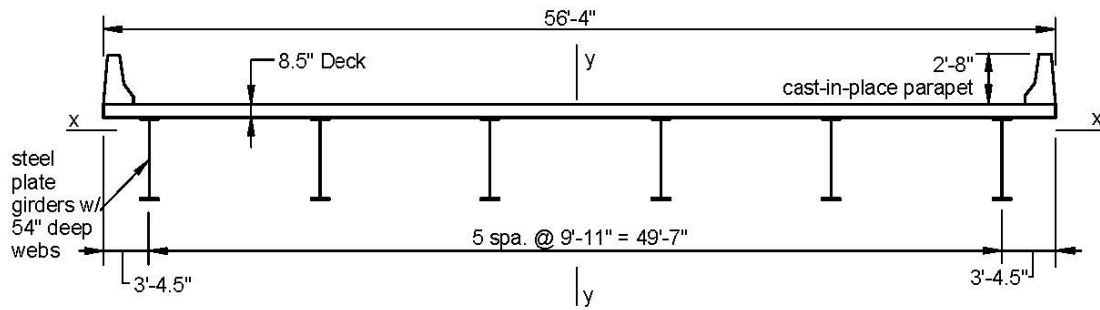


Figure 19. The simplified cross section of the East Bound bridge superstructure.

RISA 3D Model of the Bridges

The RISA 3D model of both bridges is shown in Figure 22. As mentioned earlier, for each bridge a rigid link was used to connect the superstructure and the pier cap beam. The end supports of the superstructure were modeled as fixed supports, because the beams were embedded over 2 ft-8 in into each backwall. The backwalls are supported on pile caps that connect to large wingwalls. The combination of piles and wingwalls should provide significant lateral stiffness. As mentioned for the prestressed girder bridge, abutment modeling is an area of uncertainty that could benefit from additional research.

The site class of the soil underneath the bridges was determined earlier to be class B, and spread footings were used for the foundation of this bridge. Therefore, according to Table 3 of this report, which was taken from Table 5.3.4-1 of the *LRFD Guidelines*, the support at the bottom of the columns could be considered to be rigid (fixed).

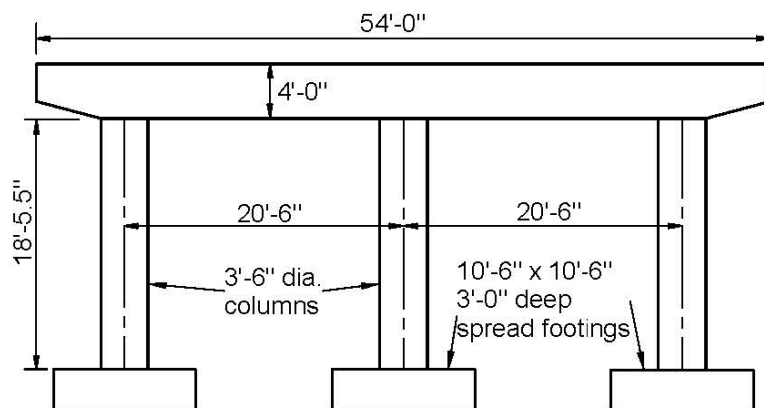


Figure 20. Simplified Pier Elevation for WB Bridge.

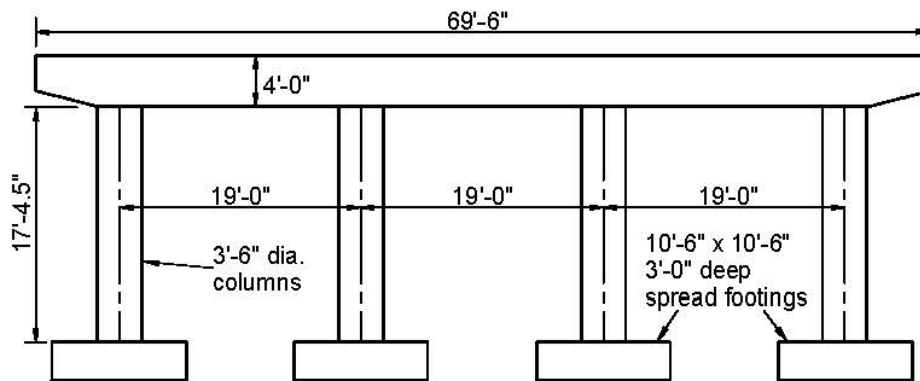


Figure 21. Simplified Pier Elevation for EB Bridge.

The joint coordinates of the bridge model were calculated according to the locations of the column center lines, pier cap beams centroidal axes and superstructure centroidal axes. The joint coordinates of the bridges are provided in Appendix II.

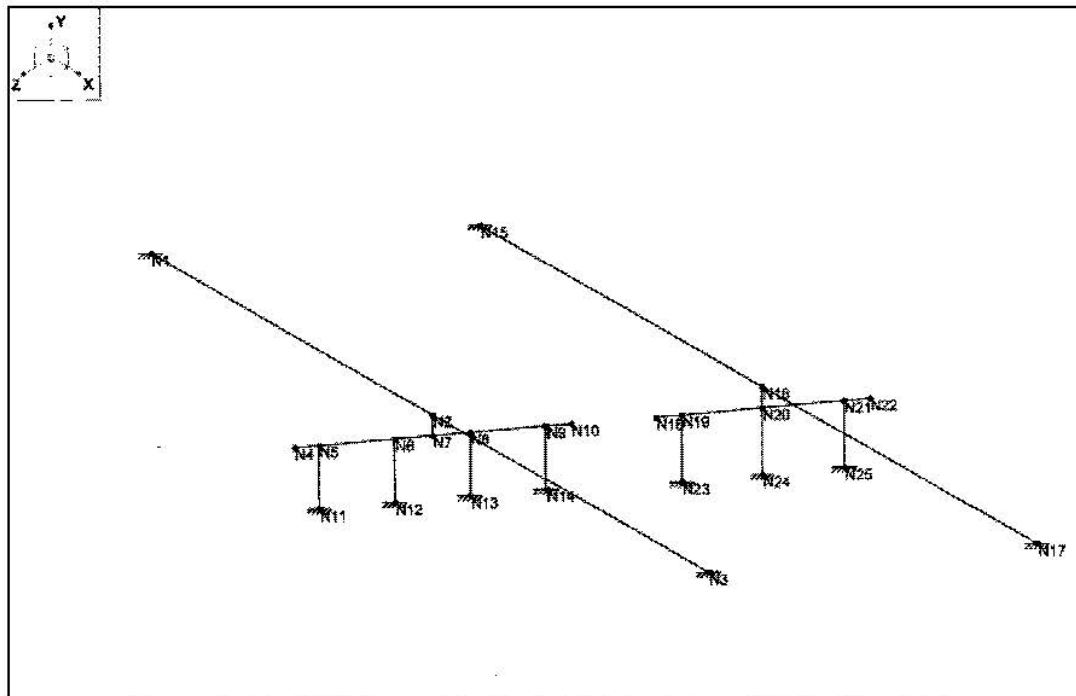


Figure 22. The RISA 3D model of the EB bridge (left) and WB bridge (right), pier is at 37 degree skew.

Dead Load Effects

The dead load effects on the pier cap beam and columns were obtained by first applying the self-weight of the superstructure plus a 20 lb/ft² allowance for construction tolerances and

construction methods as uniformly distributed loads on the superstructure (VDOT 1993). The 20 lb/ft² allowance was applied as a uniformly distributed load by multiplying it by the width of the superstructure, which is 44 ft for the WB bridge and 56 ft-4 in for the EB bridge. The model shown in Figure 22 does not produce accurate dead load effects on the pier cap beam and the columns, because the rigid link connects the midpoint of the superstructure to the midpoint of the pier cap beam, and therefore it produces erroneously high axial loads on the middle column and erroneously low axial loads on the leftmost and rightmost columns. So to more accurately model the transmission of the loads from the superstructure to the substructure, the axial load on the rigid link due to the self-weight of the superstructure and the 20 lb/ft² allowance was divided by the number of steel girders for the superstructure, which was five for the WB bridge and six for the EB bridge. Analyses were performed on the two pier structures, in which the pier cap beam was subjected to as many point loads as the number of the number of steel girders for the superstructure, plus the self-weight of the pier cap beam and the columns.

Live Load Effects

The live load effects were found by adding the maximum effects from the three moving live load cases to the lane load effects. The three moving live load cases and the lane load were shown previously in Figure 11. The case that always controlled was the third, which was the two-truck case. Each of these moving live load cases was run along the superstructure, and the largest axial load produced on the rigid link was used to run an analysis on the pier similar to that for the dead loads. The same procedure was also used to get the lane load effects.

The maximum effects of the three moving load cases, which was always the two-truck case for this bridge, was combined with the lane load effects by using the multiple presence factors (m), the dynamic load allowance (IM), and the 0.9 factor, since the controlling case was always the two-truck case (Barker and Puckett 1997). The multiple presence factors and the dynamic load allowance were presented earlier in Table 4 and Table 5, respectively.

For the West Bound bridge, which has two lanes, $m = 1.0$, while the three-lane East Bound bridge has $m = 0.85$. Since deck joints and fatigue were not the subject of interest in this analysis, $IM = 0.33$. Thus the formulas to calculate the live load effects of these bridges were:

$$LL = 1.0 \times 2 \times (1.33 \times 0.9 \times TT + 0.9 \times LN) \text{ for the WB bridge} \quad (19)$$

$$LL = 0.85 \times 3 \times (1.33 \times 0.9 \times TT + 0.9 \times LN) \text{ for the EB bridge} \quad (20)$$

TT = two-truck load effects

LN = lane load effects

Combined Dead and Live Load Effects on the Columns

The dead and live load effects were combined using the load factors from the Extreme Event-I combination presented in Equation 3. Suggested values for γ_{EQ} are 0.0, 0.5 and 1.0 (Barker and Puckett 1997). $\gamma_{EQ} = 0.5$ was chosen to reflect normal traffic loading, which assumes that there will not be excessive traffic on the bridge when an earthquake occurs. Thus the combined effects of the dead load and live load are:

$P = DL + (0.5 \times LL)$
P = combined dead load and live load effects
DL = dead load effects
LL = live load effects

The complete results of the dead load and live load effects are presented in Appendix II.

Determination of the Required Seismic Design and Analysis Procedure (SDAP) and Seismic Design Requirement (SDR)

In order to determine the required Seismic Design and Analysis Procedure (SDAP) and Seismic Design Requirement (SDR) for this pair of bridges, the following parameters must be determined:

S_s = 0.2-second period spectral acceleration, obtained from the USGS website zip code lookup for spectral accelerations at the location of the bridges
 S_1 = 1-second period spectral acceleration, obtained from the USGS website zip code lookup for spectral accelerations at the location of the bridges
 F_a = site coefficients for the short-period range, which are given in Table 6
 F_v = site coefficients for the long-period range, which are given in Table 7

This bridge is located in Tazewell County, 70 miles northeast of Bristol, in the southwestern part of Virginia. But the closest town to the bridge is Bluefield, Virginia, which has a zip code 24605. After inputting zip code 24605 into the USGS website zip code lookup for spectral accelerations, the following values were obtained:

$S_s = 0.405 \text{ g}$
 $S_1 = 0.118 \text{ g}$

Since the soil is class B, $F_a = 1.0$ and $F_v = 1.0$, therefore:

$S_{DS} = F_a S_s = (1.0)(0.405 \text{ g}) = 0.405 \text{ g}$
 $S_{D1} = F_v S_1 = (1.0)(0.118 \text{ g}) = 0.118 \text{ g}$

The values of $F_v S_1$ and $F_a S_s$ were used to determine the Seismic Hazard Level according to Table 8 of this report, which was taken from Table 3.7-1 of the *LRFD Guidelines*. When two different Seismic Hazard Levels are required by the values of $F_v S_1$ and $F_a S_s$, the higher level controls. Therefore Seismic Hazard Level III was assigned to this pair of bridges.

The Seismic Hazard Level was used to determine the required Seismic Design and Analysis Procedure (SDAP) and Seismic Design Requirement (SDR) by using Table 9 of this report, which was taken from Table 3.7-2 of the *LRFD Guidelines*. Since Seismic Hazard Level III was assigned to this pair of bridges and the operational performance objective was chosen, SDAP C, D or E could be used for this pair of bridges. But according to section 4.4.2 of the *LRFD Guidelines*, SDAP C could not be used for these two bridges because they had fewer than three spans. Thus SDAP D was required. The required Seismic Design Requirement (SDR) for

this bridge was SDR 5 according to Table 9 of this report. In the next step, the cracked section properties of the columns and pier cap beam are determined because SDAP D uses an elastic (cracked section properties) analysis.

Cracked Section Properties of the Columns

The combined axial loads from the dead and live loads were used to obtain the cracked section properties of the columns, i.e. the effective moment of inertia about the x-axis (I_{exx}) and the effective moment of inertia about the y-axis (I_{eyy}). The relationship between the axial load on the column, the reinforcement ratio and the recommended effective moment of inertia (I_e) is presented in Figure 12. For the EB bridge, I_e/I_g was approximately 0.403, while for the WB bridge, I_e/I_g was approximately 0.390. The spreadsheet for this calculation is also presented in Appendix II.

Cracked Section Properties of the Pier Cap Beam

The cracked section properties of the pier cap beam, i.e. I_{exx} and I_{eyy} , can be obtained by using either of two methods: the moment-curvature method (Priestley et al. 1996) or the method presented in the ACI 318-02 Building Code (ACI 2001). The moment-curvature relationship uses the following equation:

$$EI_e = \frac{M_y}{\phi_y} \quad (6)$$

M_y = the yield moment in the moment-curvature relationship for the cross section
 ϕ_y = the yield curvature in the moment-curvature relationship for the cross section

The cracked section properties using this method produced $I_e = 0.305 I_g$ for the WB pier cap beam, and $I_e = 0.327 I_g$ for the EB pier cap beam. The complete calculation for this method is presented in Widjaja (2003).

Using the ACI method revealed that the pier cap beam was not expected to be cracked at service loads, since $M_{cr} > M_a$ (the maximum positive or negative moment in the pier cap beam), and therefore $I_e = I_g$.

Despite the discrepancy between the result of the moment-curvature method and the ACI Equation, the moment-curvature result was used. As with the previous example, it was assumed that there would be some cracking in the cap due to other effects.

Section Properties of the Superstructure

The superstructure's gross section properties were used for the analysis of the bridge. After completion of the analysis of the structure subjected to the equivalent earthquake load, the assumption was checked by comparing the maximum moment in the superstructure to the cracking moment. The assumption of uncracked properties was shown to be correct. The calculations for this analysis are provided in Widjaja (2003).

Period of Vibration

After obtaining the cracked section properties for the pier cap beam and the columns, the RISA 3D model of the bridge was modified by changing the gross section properties to the effective section properties. The next step was to compute the period of vibration of the bridge. For comparison, two methods were used to calculate the period of vibration, the uniform load method and the single mode spectral analysis method (MCEER 2001).

Uniform Load Method

The uniform load method is an equivalent static method of analysis that uses a uniform lateral load to approximate the effect of seismic loads. The method is suitable for common bridges that respond primarily in their fundamental mode of vibration.

The first step of this method was to apply a uniformly distributed load p_0 , which can be set arbitrarily to any magnitude according to one's preference, over the length of the bridge. For this bridge analysis, p_0 was set to 100 kips/in so that the resulting deflections would have a reasonable magnitude. For this bridge, p_0 was applied only in the transverse direction. Since the bridge has integral abutments, it was assumed that the bridge superstructure and substructure would move together in an earthquake in the longitudinal direction. Each span of the bridge was divided into sections, eleven in this case, and the lateral displacement of each section was called $v_s(x)$. The bridge lateral loading is shown in Figure 23.

Based on the output from the RISA analysis, the bridge lateral stiffness (K) and total weight (W) were calculated by using equations 7 and 8.

$$K = \frac{p_0 L}{v_{s,MAX}} \quad (7)$$

L = total length of the bridge = 2352 in (EB) and 2344 in (WB)

$v_{s,MAX}$ = maximum value of $v_s(x)$ = 5.34 in (EB) and 10.37 in (WB)

K = 44045 k/in for the EB bridge

K = 22601 k/in for the WB bridge

$$W = \int w(x) dx \quad (8)$$

$w(x)$ = weight per unit length of the dead load of the bridge superstructure and tributary substructure

W = 1897 kips for the EB bridge

W = 1515 kips for the WB bridge

The fundamental period of vibration was calculated as follows:

$$T = 2\pi \sqrt{\frac{W}{gK}} \quad (9)$$

g = acceleration of gravity = 386 in/sec²

T = 0.0828 sec. for the WB bridge

T = 0.0664 sec. for the EB bridge

Single Mode Spectral Analysis Method

The primary difference between this method and the uniform load method is that the equivalent lateral earthquake forces for this method are not uniformly distributed loads over the length of the bridge. The magnitude varies over the length of the bridge, as a function of the lateral displacement at each point. The complete calculation of the period of vibration using the single mode spectral analysis method is presented in Widjaja (2003).

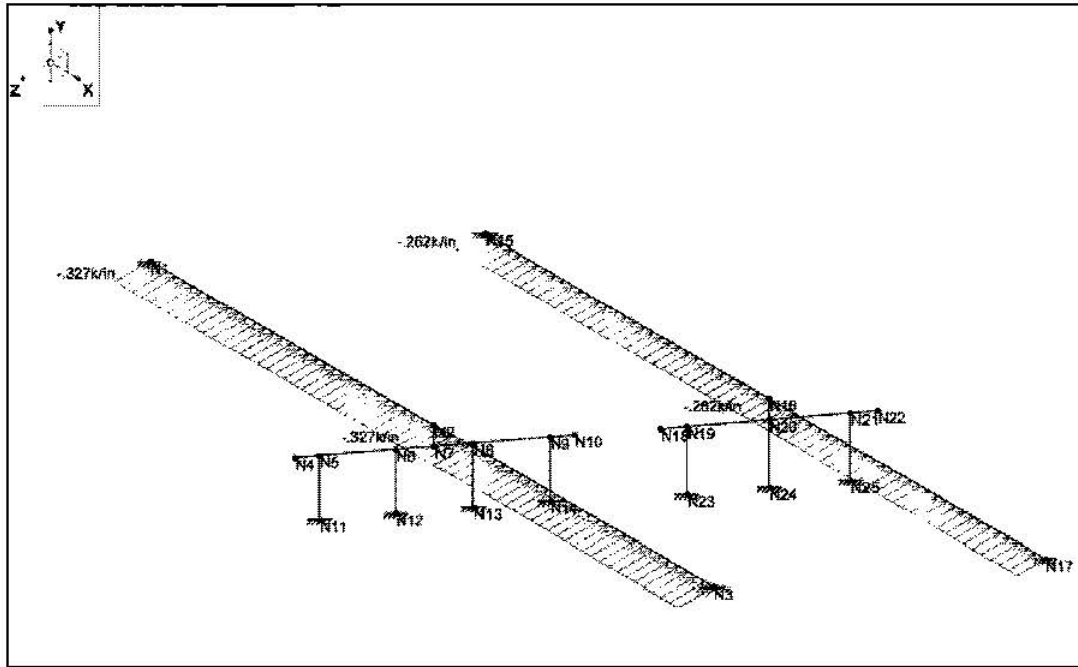


Figure 23. The uniform lateral loading on the bridge.

As in the uniform load method, first the bridge was subjected to a uniform load p_o of 100 kips/in, and the resulting deflection of each of the eleven sections as given by RISA 3D was called $v_s(x)$. Then the α , β , and γ factors were calculated as follows:

$$\alpha = \int v_s(x) dx \quad (10)$$

$$\beta = \int w(x)v_s(x) dx \quad (11)$$

$$\gamma = \int w(x)v_s(x)^2 dx \quad (12)$$

$w(x)$ = the weight of the dead load of the bridge superstructure and tributary superstructure.

For the WB bridge,

$$\alpha = 12986 \text{ in}^2$$

$$\beta = 7662 \text{ kip-in}$$

$$\gamma = 63585 \text{ kip-in}^2$$

For the EB bridge,

$$\alpha = 6709 \text{ in}^2$$

$$\beta = 4922 \text{ kip-in}$$

$$\gamma = 21069 \text{ kip-in}^2$$

Then the period of the bridge can be calculated from the expression:

$$T = 2\pi \sqrt{\frac{\gamma}{p_o g \alpha}} \quad (13)$$

$$T = 0.0708 \text{ sec. for the WB bridge.}$$

$$T = 0.0567 \text{ sec. for the EB bridge.}$$

Design Response Spectrum Curve

After the periods of vibration were determined, the next step was to draw the design response spectrum curve, from which the spectral acceleration (S_a) can be obtained. The required values for the generation of the curve are as follows:

$$S_{DS} = 0.405 \text{ g}$$

$$S_{DI} = 0.118 \text{ g}$$

$$T_s = \frac{S_{DI}}{S_{DS}} = \frac{0.118 \text{ g}}{0.405 \text{ g}} = 0.291 \text{ sec} \quad (14)$$

$$T_o = 0.2 T_s = 0.2 (0.291 \text{ second}) = 0.0583 \text{ sec} \quad (15)$$

(MCEER 2001).

The design response spectrum curve for this example is given in Figure 24.

It can be seen from Figure 24 that for $T = 0.0828 \text{ sec}$ or 0.0708 sec (WB bridge) and $T = 0.0664 \text{ sec}$ (EB bridge), $S_a = 0.405 \text{ g}$. The period of vibration for the EB bridge using the single mode spectral analysis method was 0.0567 sec which lies on the segment of the design response spectrum curve for which very short period structures have smaller spectral accelerations. However, the 0.0567 sec period was very close to the 0.058 sec period that marks the start of the plateau region of the curve. Hence, $S_a = 0.405 \text{ g}$ was used as a conservative value.

Equivalent Earthquake Forces

After obtaining the spectral acceleration from the design response spectrum curve, the equivalent earthquake forces were computed. The equivalent earthquake forces can be computed using either the uniform load method or the single mode spectral analysis method (MCEER 2001).

Uniform Load Method

The equivalent earthquake force, p_e , was calculated using the expression:

$$p_e = \frac{S_a W}{L} \quad (16)$$

S_a = the spectral acceleration from the design response spectrum curve (MCEER 2001).

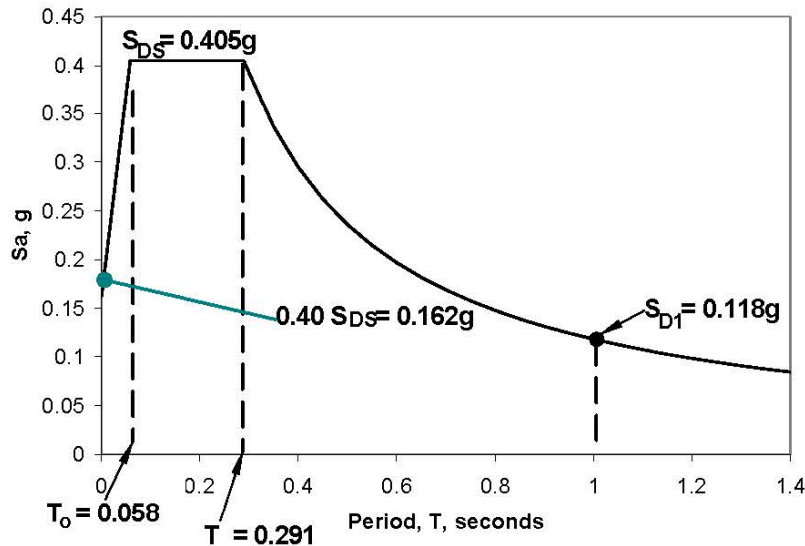


Figure 24. The design response spectrum curve for the Tazewell County bridges.

For the West Bound bridge, $p_e = 3.14$ kip/ft, and for the East Bound bridge, $p_e = 3.92$ kip/ft.

Single Mode Spectral Analysis Method

The equivalent earthquake force computed using this method is not a uniformly distributed load as in the uniform load method. Instead the lateral earthquake load varies with mass and displacement along the length of the structure. The equivalent earthquake force, p_e , was calculated using the expression:

$$p_e(x) = \frac{\beta S_a}{\gamma} w(x) v_s(x) \quad (17)$$

$p_e(x)$ = the equivalent earthquake force for that section
Other variables as defined previously.

Since each span of the bridge was divided into eleven sections and each section of the span had a different deflection $v_s(x)$, each section also had a different equivalent earthquake force. The equivalent earthquake loadings for the two bridges using this method are shown in Figures 25 and 26. The distributed load in the middle is much larger than the other distributed loads, because the distributed load in the middle carries the tributary load of the substructure. The complete calculation to compute the equivalent earthquake force using this method is presented in Widjaja (2003).

Combined Effects of the Dead, Live and Earthquake Loads

The final analysis of the bridge was performed using the cracked section properties for dead, live and earthquake loads. The procedure to calculate the dead and live load effects for this final analysis is the same as that used to perform the analysis to calculate the dead and live load effects to obtain cracked section properties. For the earthquake loads, the axial loads, moments and shears for the pier cap beam and columns were taken directly from the analysis on the entire bridge. The load factors used to combine the dead, live and earthquake load effects are given in Equation 3 (Extreme Event-I). But for the earthquake loads, the responses (axial loads, moments and shears) were divided by the R factor given in Table 10. Since SDAP D (Elastic Response Spectrum Method) and the Operational performance level were used in this research study, the earthquake load responses on the columns were divided by $R = 1.5$. Thus the combined effects of the dead, live and earthquake loads are given by the following expression:

$$P = 1.0DL + 0.5LL + 1.0\left(\frac{EQ}{1.5}\right) \quad (18)$$

The complete results of the dead, live and earthquake load effects are given in Appendix II.

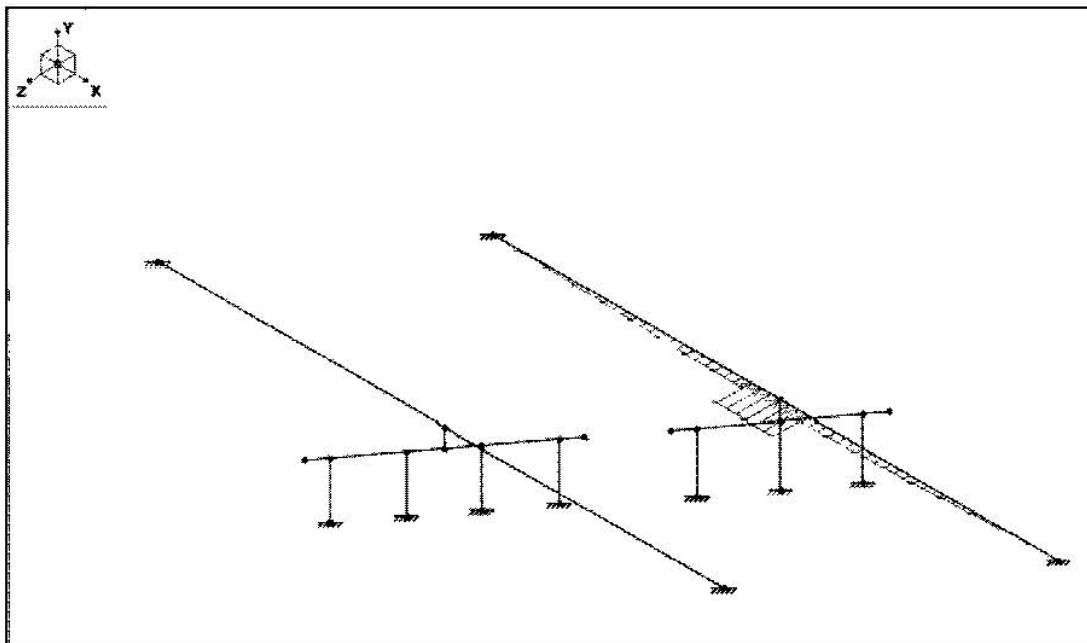


Figure 25. The segmentally uniform loading of the West Bound bridge

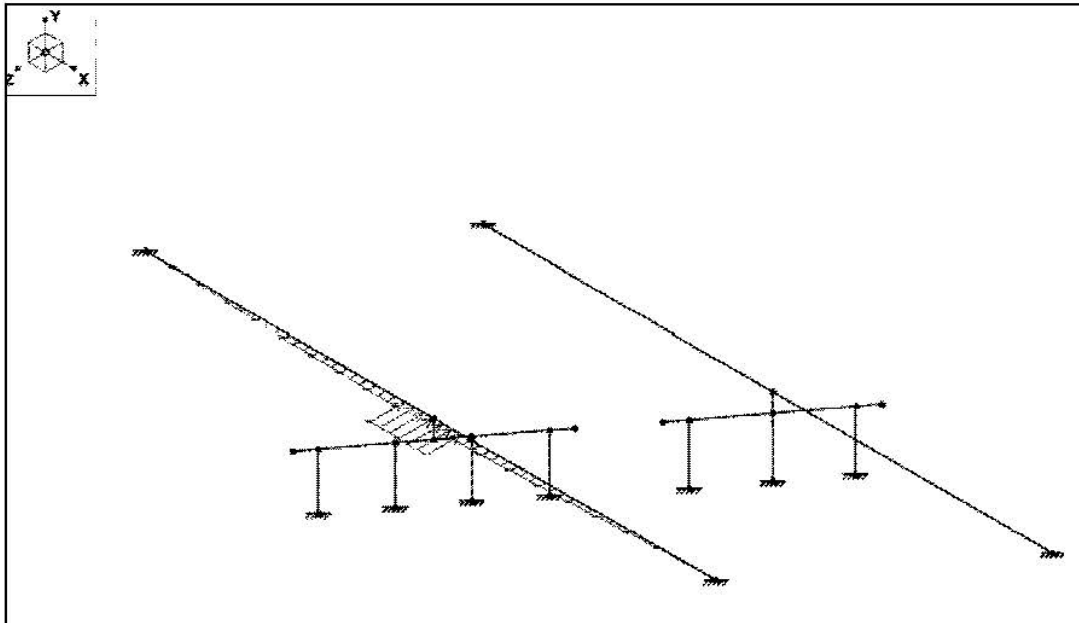


Figure 26. The segmentally uniform loading of the East Bound bridge.

Column Strength under Flexure and Axial Loads

The interaction diagram of the columns was constructed to determine if the combinations of axial load and moment exceeded the capacity of the column. The complete calculation of the points of the interaction diagram is provided in Widjaja (2003). For all the columns of these two bridges, the maximum axial load and moment were far below the capacity of the column, as shown in Figures 27 and 28.

Flexural Strength of the Pier Cap Beam

The flexural strength of the pier cap beam was calculated for each bridge and compared to the maximum factored moments in the pier cap beams. In order to simplify the calculation of the flexural strength, the side reinforcing bars of the pier cap beam were ignored. The simplified cross sections of the caps are shown in Figures 29 and 30. The complete calculations of the flexural strengths of the pier cap beams are presented in Widjaja (2003).

West Bound:

$$\phi M_n = 2674 \text{ k-ft}$$

$$M_u = 552 \text{ k-ft}$$

$$\phi M_n > M_u$$

East Bound:

$$\phi M_n = 2174 \text{ k-ft}$$

$$M_u = 516 \text{ k-ft}$$

$$\phi M_n > M_u$$

Thus the flexural capacity of the pier cap beam was not exceeded for either bridge.

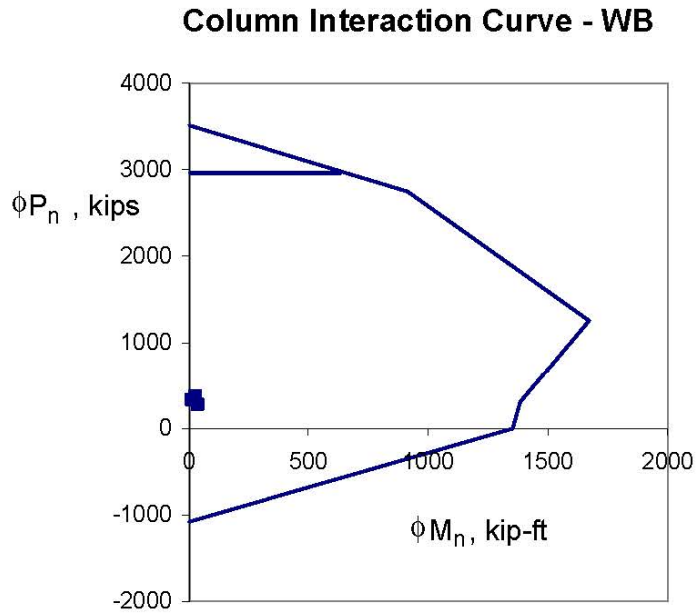


Figure 27. The interaction diagram of the West Bound bridge columns (42 in diameter column with 20 No. 9 bars). The points are the factored axial loads and moments in the columns.

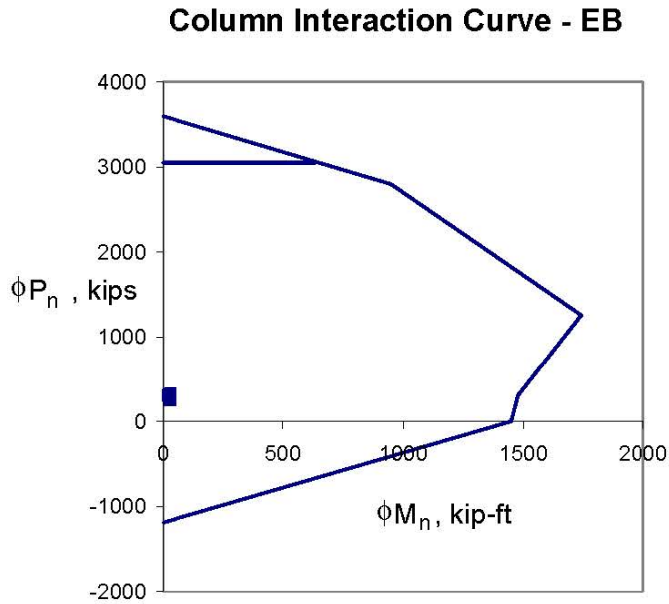


Figure 28. The interaction diagram for the East Bound bridge columns (42 in diameter column with 22 No. 9 bars). The points are the factored axial loads and moments in the columns.

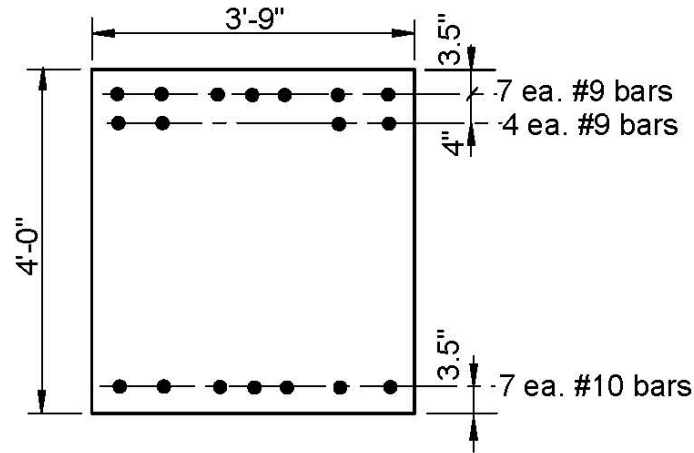


Figure 29. The simplified cross section of the West Bound bridge pier cap beam.

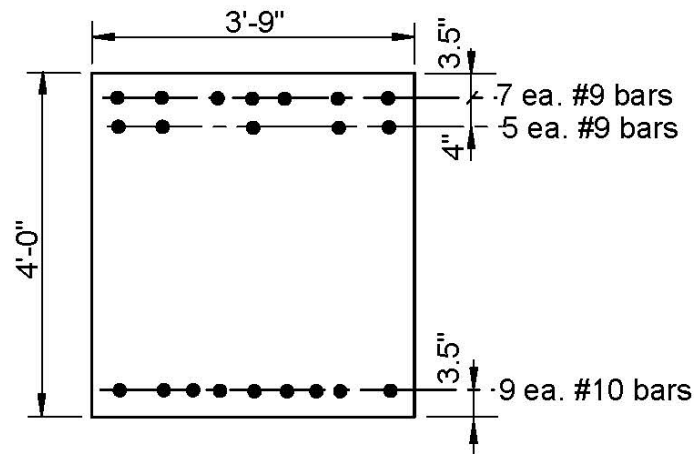


Figure 30. The simplified cross section of the East Bound bridge pier cap beam.

Detailing Changes Due to the New LRFD Guidelines

The details of the two bridges were checked according to the required Seismic Design Requirement, which was SDR 5 for these two bridges. The summaries of the checks for the West Bound and East Bound bridges are given in Tables 13 and 14 respectively. Also the calculated maximum lateral displacements of the bridges were examined and found to be extremely small at 0.03 in for the WB and 0.02 in for the EB bridge.

The critical detailing checks involve the spiral reinforcement in the columns and in the beam-column and footing-column joints. The reinforcing must be checked to ensure that it provides adequate confinement to the core, provides adequate shear strength, and provides adequate bracing to prevent the longitudinal bars from buckling.

Using current *Standard Specifications* seismic design provisions and peak ground acceleration maps, the existing design is adequate. The peak ground acceleration is 7.5%. If the bridge is assumed essential, it is classified as Seismic Performance Category A (SPC A). For SPC A the bearing seat length must be checked and the connection between the superstructure and substructure must be designed to carry 20% of the tributary weight of the structure. There are no other detailing requirements. Therefore, this bridge is adequate according to the *Standard Specifications*.

Table 13. The results of the detailing requirement checks for the West Bound bridge using SDR 5.

Number	Requirement	Required	Provided
1a	Transverse Reinforcement in Potential Plastic Hinge Zones using the Implicit Shear Detailing Approach	0.00135	0.000572
1b	Transverse Reinforcement outside the Plastic Hinge Zones using the Implicit Shear Detailing Approach	minimum	0.000572
3	Transverse Reinforcement for Confinement at Plastic Hinges	0.00297	0.00114
4	Spiral Spacing for Longitudinal Bar Restraint at Plastic Hinges	6.77 in	10.5 in
5	Spiral Spacing for Confinement at Plastic Hinges	4 in	10.5 in
6	Transverse Spiral Reinforcement at the Moment Resisting Connection Between Members (Column/Beam and Column/Footing Joints) using explicit approach	0.00478	0.00114
7	Minimum Required Horizontal Reinforcement	0.00478	0.00114
8	Stirrups in the Pier Cap Beam within Half of the Cap Depth on Either Side of the Column	3.2 in ²	7.44 in ² for the left and right columns, and 4.96 in ² for the center column
9	Lap Splices at the Top and Bottom One-quarter of the Column	Not Allowed	Used
10	Column Joint Spiral Reinforcement to be Carried into the Pier Cap Beam	0.00584	0

Table 14. The results of the detailing requirement checks for the East Bound bridge using SDR 5.

Number	Requirement	Required	Provided
1a	Transverse Reinforcement in Potential Plastic Hinge Zones using the Implicit Shear Detailing Approach	0.00155	0.000572
1b	Transverse Reinforcement outside the Plastic Hinge Zones using the Implicit Shear Detailing Approach	minimum	0.000572
3	Transverse Reinforcement for Confinement at Plastic Hinges	0.00339	0.00114
4	Spiral Spacing for Longitudinal Bar Restraint at Plastic Hinges	6.77 in	10.5 in
5	Spiral Spacing for Confinement at Plastic Hinges	4 in	10.5 in
5	Transverse Spiral Reinforcement at the Moment Resisting Connection Between Members (Column/Beam and Column/Footing Joints) using explicit approach	0.00478	0.00114
6	Minimum Required Horizontal Reinforcement	0.00478	0.00114
7	Stirrups in the Pier Cap Beam within Half of the Cap Depth on Either Side of the Column	3.52 in ²	7.44 in ² for all the columns
8	Lap Splices at the Top and Bottom One-quarter of the Column	Not Allowed	Used
9	Column Joint Spiral Reinforcement to be Carried into the Pier Cap Beam	0.00584	0

To bring these two bridges up to the new standards, the spiral spacing must be changed from a No. 3 spiral with a 10.5 in pitch to a No. 5 spiral at a 4 in pitch. Also, the spiral must be carried up through the full height of the cap and down into the footing. This results in an additional 4800 lb of reinforcing steel in the bridge, which will result in an approximately 0.3% increase in the total construction cost. The complete detailing requirements and cost increase calculations are presented in Widjaja (2003).

Parametric Study

Objective

The objective of this parametric study was to examine common substructure configurations to determine the influence of the new *LRFD Guidelines* on column longitudinal and transverse (confinement) reinforcement. A simple two span bridge with a three column center bent was chosen for the study. The span lengths and column heights were varied. Three bridge locations, Northern Virginia, the Richmond area and the Bristol area, were examined for two soil conditions, Class B and Class D.

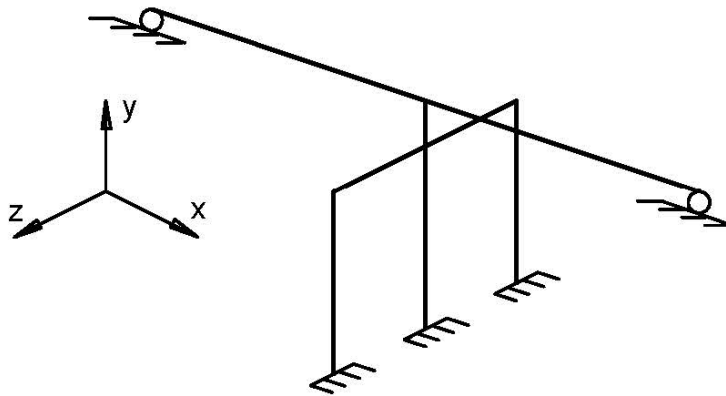


Figure 31. The RISA 3D model of the bridge used in the parametric study.

Bridge Structure

The RISA 3D model of the bridge is shown in Figure 31. In this model, unlike the RISA 3D models for the previously analyzed bridges, the longitudinal (x-direction) supports at the abutments were released. Thus the model represents a bridge with sliding bearings, which allow longitudinal movement (x-direction), at the abutments. In the transverse direction the abutments were pinned for the soil Class B study. For soil Class D, two extreme situations were examined: a pinned condition and a free-to-translate condition. In reality the abutment would be modeled with a spring whose stiffness reflected the stiffness of the piles beneath the abutment and the soil surrounding it. The actual loads to the center bent should fall somewhere between the cases of pinned and free abutments.

The section properties of the superstructure used in this parametric study were taken from the average section properties of the two steel girder bridges (West Bound and East Bound) analyzed in the previous section. The I_{yy} value is a weighted average assuming a bridge width of 50 ft. Therefore, the section properties for the superstructure in this parametric study are:

$$Area = (West\ Bound\ Area + East\ Bound\ Area) / 2$$

$$Area = \frac{899in^2 + 1114in^2}{2}$$

$$Area \approx 1007in^2$$

$$I_{xx} = (West\ Bound\ I_{xx} + East\ Bound\ I_{xx}) / 2$$

$$I_{xx} = \frac{373,000in^4 + 521,000in^4}{2}$$

$$I_{xx} = 447,000in^4$$

$$I_{yy} = ((West\ Bound\ I_{yy} / W^3 + East\ Bound\ I_{yy} / W^3) / 2) * 50^3$$

$$I_{yy} = \frac{25,600,000in^4 / (44^3) + 50,500,000in^4 / (56^3)}{2} (50^3)$$

$$I_{yy} = 36,700,000in^4$$

The substructure used in this parametric study is shown in Figure 32. The bent has three 36-in-diameter columns at 20 ft center-to-center. The pier cap beam is 45 in wide and 50 in deep. The height of the columns was one of the parameters in this study, and the three different column heights were 20 ft, 30 ft and 40 ft. For the columns, f_c was 3600 psi. The reinforcement ratio for each column was 1.5%. The bridge had two spans, and the span length was also a parameter in this study. The six different span lengths were 80 ft, 90 ft, 100 ft, 110 ft, 120 ft and 140 ft.

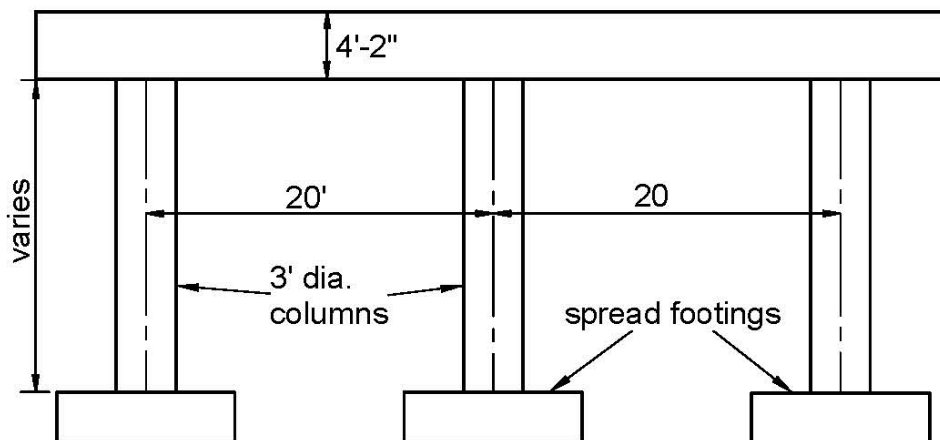


Figure 32. Substructure of the bridge used in this parametric study.

Bridge Stiffness

All the calculations for this parametric study are provided in Widjaja (2003). To determine the periods of vibration of the two bridges, the stiffness values of the bridges in the transverse and longitudinal directions were determined. The stiffness in the transverse direction was obtained by applying a force P to the substructure as shown in Figure 33. Cracked section properties were used for the columns. To calculate the cracked section properties, the superstructure was assumed to be 10 kips/ft, and the weight of the pier cap beam was assumed to be 120 kips. The ratio $P/(f_c' A_g)$ was calculated for each combination of span length and column height. Then the ratio I_e/I_g , which was obtained from using the ratio $P/(f_c' A_g)$ and Figure 12, was also calculated for each combination of span length and column height. The six different I_e/I_g ratios for every column height were averaged and the I_e average was used for all the columns of the six bridge models with that column height to determine the stiffness in the transverse direction. The cap was assumed to be cracked with the effective I assumed to be $0.35I_g$. The stiffness in the transverse direction was calculated by using Equation 19:

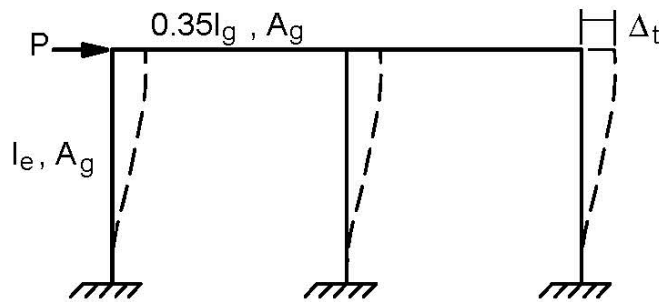


Figure 33. The loading to the substructure to determine the stiffness in the transverse direction.

$$K_{tb} = \frac{P}{\Delta_t} \quad (19)$$

K_{tb} = the stiffness in the transverse direction

P = the magnitude of the force in the transverse direction

Δ_t = the deflection in the transverse direction

The stiffness in the longitudinal direction was obtained by applying the force P to a single cantilever column, whose section properties represent that of the three columns of the substructure. This is shown in Figure 34. The stiffness in the longitudinal direction was calculated by using equation 20:

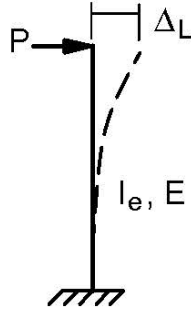


Figure 34. The loading to the substructure, modeled as a cantilever column, to determine the stiffness in the longitudinal direction.

$$K_L = \frac{P}{\Delta_L} = \frac{3EI_e}{L^3} \quad (20)$$

- K_L = the stiffness in the longitudinal direction
- P = the magnitude of the force in the longitudinal direction
- Δ_L = the deflection in the longitudinal direction
- E = the modulus of elasticity of concrete
- I_e = the total cracked moment of inertia of the three columns of the substructure
- L = the length (height) of the cantilever column
= height of the column + (0.5 × pier cap beam height)

Equation 20 comes from the deflection formula for a cantilever column, which is:

$$\Delta_L = \frac{PL^3}{3EI} \quad (21)$$

Periods of Vibration

The periods of vibration in the transverse and longitudinal were determined for each combination of span length and column height.

The period of vibration in the transverse direction for the cases where the abutments were prevented from translating was determined by using the configuration shown in Figure 35. A 1 kip/ft uniformly distributed load was applied to a simply-supported two-span bridge with a spring, which has stiffness of K_{tb} defined in the previous section, attached to the midpoint of the bridge. The maximum deflection, Δ_{max} , was then used to calculate the period of vibration in the transverse direction using Equation 22:

$$T_{tp} = 2\pi \sqrt{\frac{W}{gK_t}} \quad (22)$$

- T_{tp} = period of vibration in the transverse direction with abutments pinned
- W = weight of the superstructure and pier cap beam (columns excluded)

$g = \text{gravitational acceleration} = 386 \text{ in/sec}^2$

$$K_t = \frac{(1k/ft)(2l)}{\Delta_{\max}}$$

$l = \text{length of one span of the bridge}$

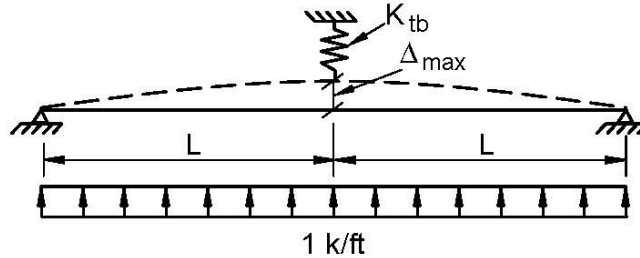


Figure 35. The loading to obtain the period of vibration of the bridge in the transverse direction with abutments pinned.

To determine the period of vibration for the case in which the abutments were free to translate laterally, only the stiffness of the center bent was considered as follows:

$$T_{tf} = 2\pi \sqrt{\frac{W}{gK_{tb}}} \quad (23)$$

$T_{tf} = \text{period of vibration in the transverse direction with abutments free}$

The period of vibration in the longitudinal direction was calculated using equation 24 for each combination of span length and column height.

$$T_L = 2\pi \sqrt{\frac{W}{gK_L}} \quad (24)$$

$W = \text{weight of the superstructure and pier cap beam (columns excluded)}$

$g = \text{gravitational acceleration} = 386 \text{ in/sec}^2$

$K_L = \text{bridge stiffness in the longitudinal direction}$

The periods of vibration in the transverse directions, with abutments pinned and free, and longitudinal directions for each combination of span length and column height are given in Tables 15, 16 and 17, respectively.

It is important to note that the height of the columns made very little difference for the period of vibration in the transverse direction with the abutments pinned. This was the case because in this parametric study, the bridge was modeled with the superstructure very stiff compared to the piers. The superstructure is approximately 50 ft wide and between 160 ft and 280 ft long from abutment to abutment. Multi-span structures, in which the overall length of the

structure is much greater, will be more influenced by the stiffness of the substructure, when the abutments are pinned.

The periods of vibration in the longitudinal direction are very high. This was the case because K_L , the bridge stiffness in the longitudinal direction, is very low because all stiffness is provided by the pier bending about its weak axis.

Table 15. The periods of vibration in the transverse direction with abutments pinned(sec)

		Column Height		
		20 ft	30 ft	40 ft
Span Length	80 ft	0.122	0.123	0.123
	90 ft	0.153	0.155	0.155
	100 ft	0.186	0.190	0.191
	110 ft	0.223	0.228	0.230
	120 ft	0.262	0.270	0.272
	140 ft	0.347	0.363	0.368

Table 16. The periods of vibration in the transverse direction with the abutments free(sec)

		Column Height		
		20 ft	30 ft	40 ft
Span Length	80 ft	0.92	1.59	2.37
	90 ft	0.98	1.68	2.50
	100 ft	1.03	1.77	2.63
	110 ft	1.07	1.85	2.75
	120 ft	1.12	1.93	2.87
	140 ft	1.20	2.07	3.09

Table 17. The periods of vibration in the longitudinal direction (sec)

		Column Height		
		20 ft	30 ft	40 ft
Span Length	80 ft	1.75	3.07	4.61
	90 ft	1.85	3.24	4.87
	100 ft	1.95	3.41	5.12
	110 ft	2.04	3.56	5.35
	120 ft	2.12	3.71	5.58
	140 ft	2.28	4.00	6.01

Equivalent Earthquake Loads

To determine the equivalent earthquake loads, the design response spectrum curves were drawn. This parametric study investigated the effects of earthquake loads in three locations: Vienna, VA, where the seismic risk is low, Richmond, VA, where the seismic risk is moderate, and Bristol, VA, where the seismic risk is high. Soil classes B and D were examined in the three locations. The design response spectrum curves at Vienna, Richmond and Bristol for soil class B are shown in Figures 36, 37 and 38, and for soil class D are shown in Figures 39, 40 and 41.

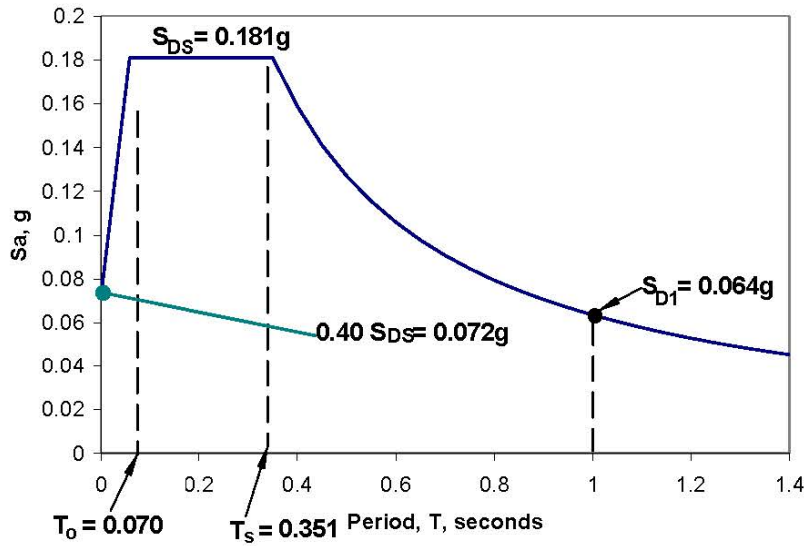


Figure 36. The Design Response Spectrum Curve for Vienna, VA, Soil Class B.

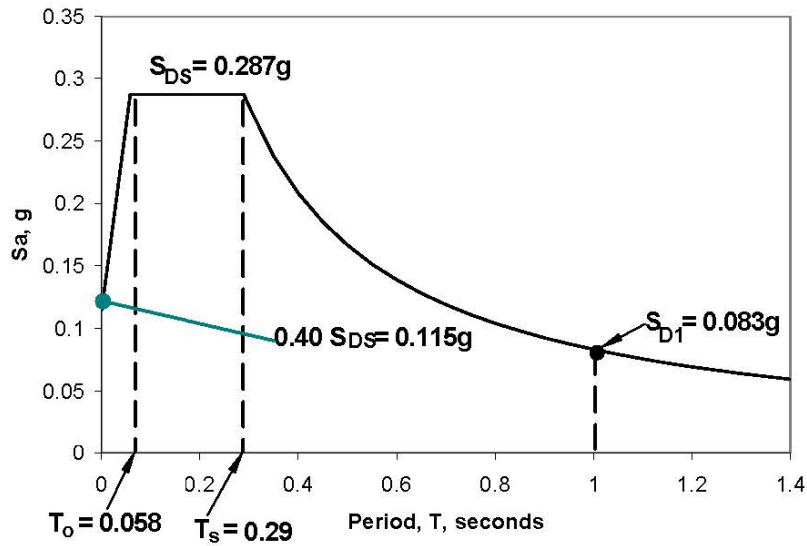


Figure 37. The Design Response Spectrum Curve for Richmond, VA, Soil Class B.

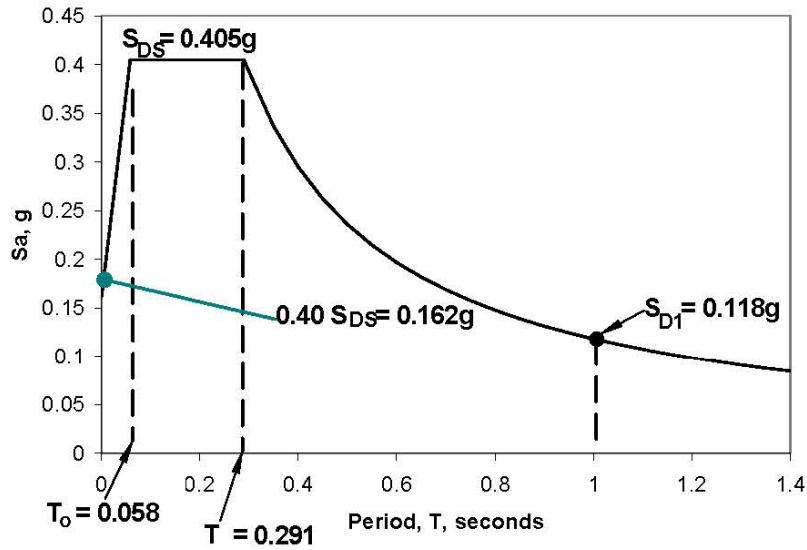


Figure 38. The Design Response Spectrum Curve for Bristol, VA, Soil Class B.

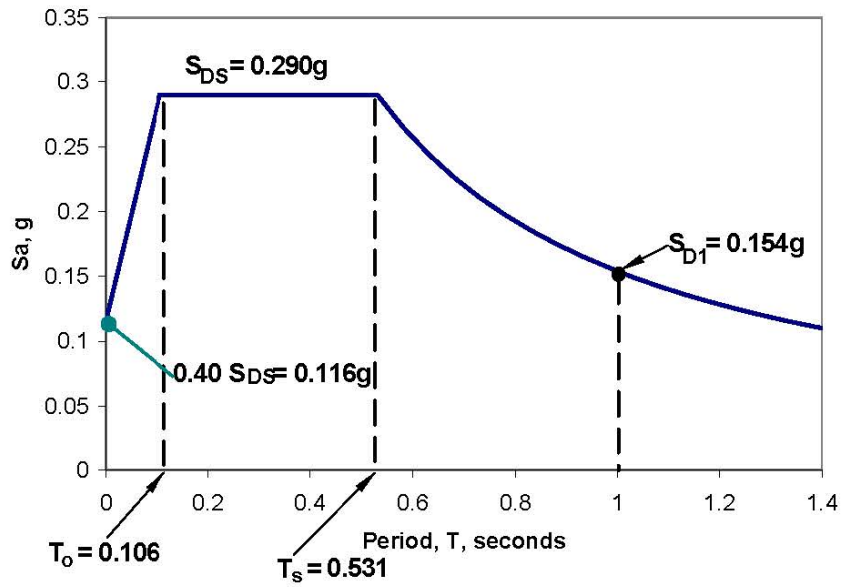


Figure 39. The Response Spectrum Curve for Vienna, VA, Soil Class D.

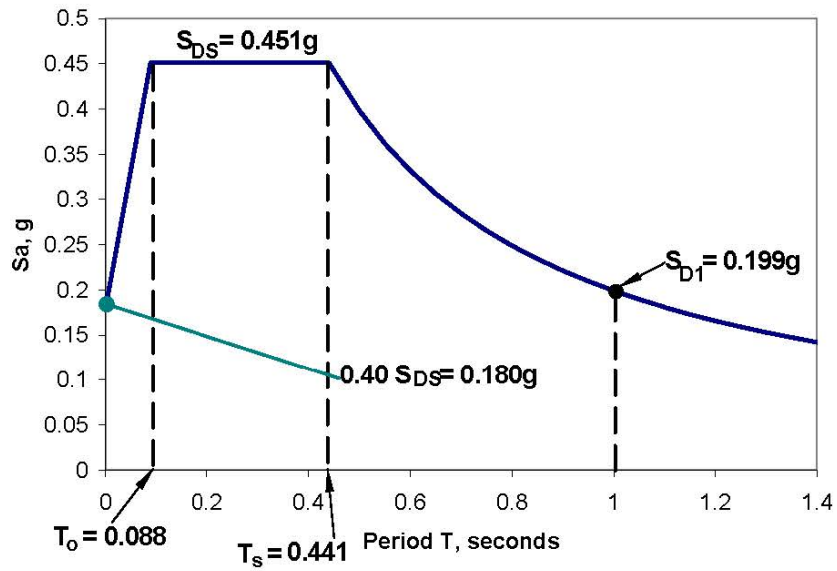


Figure 40. Response Spectrum Curve for Richmond, VA, Soil Class D.

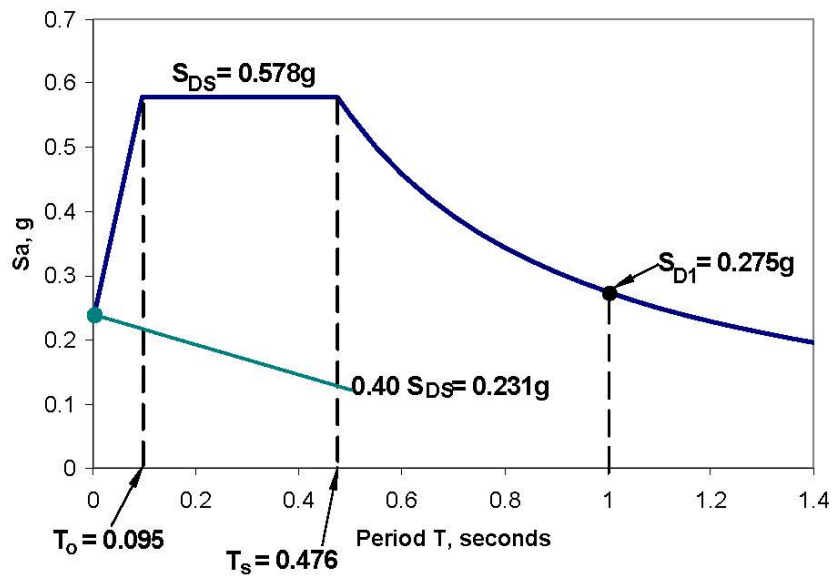


Figure 41. Response Spectrum Curve for Bristol, VA, Soil Class D.

The equivalent earthquake loads in the transverse direction were calculated for every span length, column height and soil class at every location (Vienna, Richmond and Bristol) by using equation 16:

$$p_e = \frac{S_a W}{L} \quad (16)$$

p_e = equivalent earthquake load in the transverse direction
 S_a = spectral acceleration from the design response spectrum curve
 W = weight of the superstructure and the pier cap beam
 L = the length of the bridge

The equivalent earthquake loads in the longitudinal direction were calculated for each combination of span length, column height and soil class at every location by using Equation 25:

$$P = S_a W \quad (25)$$

P = equivalent earthquake load in the longitudinal direction
 S_a = spectral acceleration from the design response spectrum curve
 W = weight of the superstructure and the pier cap beam

Column Flexural Strength

The column moment and axial load were calculated for each combination of span length, column height and soil class at all three locations (Vienna, Richmond and Bristol) by using equation 25:

$$P = 1.0DL + 0.5LL + 1.0 \frac{EQ}{R} \quad (25)$$

P = the total combined effects from dead, live and earthquake loads
 DL = the dead load effects
 LL = the live load effects
 EQ = the earthquake load effects
 R = the base response modification factor from Table 10 = 1.5

The responses in the two orthogonal directions were combined using the recommendations of the *LRFD Guidelines*. This required examining two possible combinations of earthquake effects: 40% of the longitudinal effect plus 100% of the lateral and 100% of the longitudinal effect plus 40% of the lateral. The vector sum of these two effects plus the dead and live load effects were compared to determine the worst case combination.

The column moments and axial loads were plotted and compared to the column interaction diagram. The comparisons for Vienna, Richmond and Bristol are shown in Figures 42, 43 and 44, respectively. As the three figures show, all the Vienna, Richmond and Bristol bridges with 1.5% column reinforcement are adequate to sustain the design dead, live and

earthquake loads for soil class B. For soil class D, if the abutments can provide some contribution to the lateral stiffness of the system, then for most cases a 2.5% column reinforcement ratio will be adequate. In Richmond and Bristol, if the springs at the abutments are very flexible, the column longitudinal reinforcement will have to be increased significantly, or the column size will need to be increased. However, this must be done with caution, because as the stiffness of the center pier increases, the load it draws increases as well.

In summary, for the case where the abutments were prevented from translating laterally, the periods of vibration in the transverse direction were not greatly affected by the height of the columns, but they increased as the bridge spans became longer. As explained earlier, that was the case because the bridge was modeled with the superstructure much stiffer than the columns. The periods of vibration in the longitudinal direction and in the transverse direction when the abutments were free to translate increased as the columns became taller, and as the bridge spans became longer.

With a 1.5% reinforcement ratio, all the columns had enough longitudinal reinforcement in all locations for soil class B. In this parametric study, unlike the previous bridges, the longitudinal constraints (x-direction) at the ends of the superstructure (at the abutments) were released with the use of sliding bearings, which made the columns sustain higher loads from the earthquake forces in the longitudinal direction.

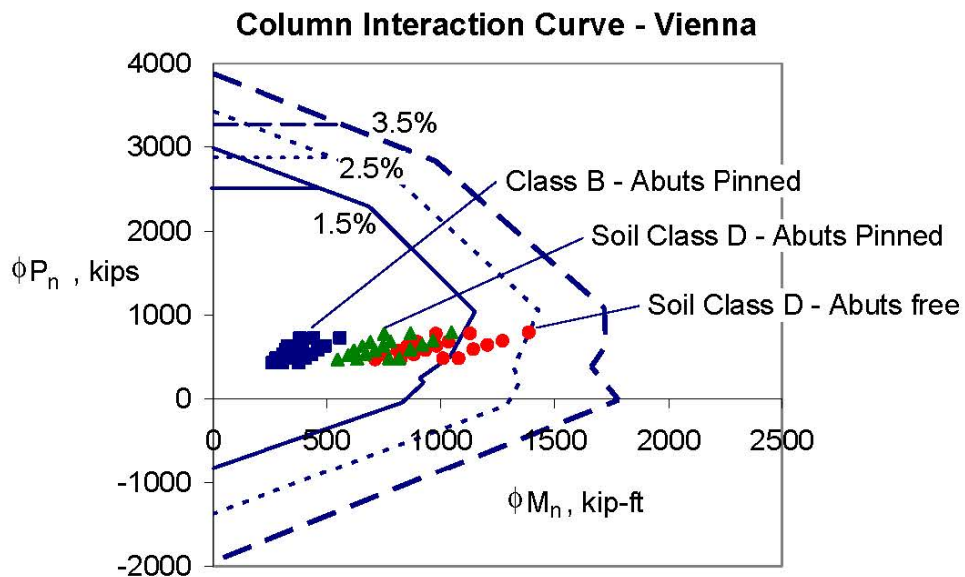


Figure 42. The comparison between the column interaction diagram and the axial loads and moments of the column for Vienna, VA. The points are the factored axial loads and moments in the columns.

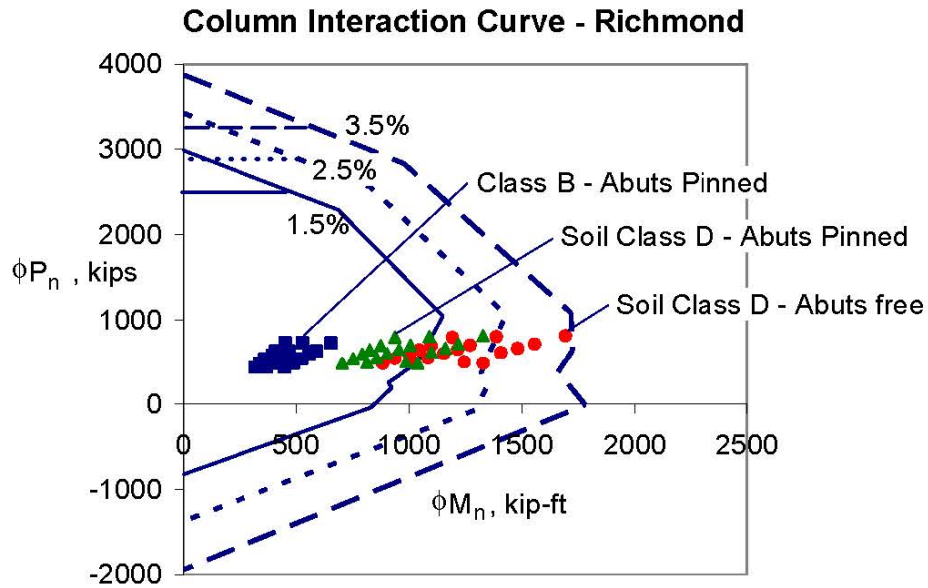


Figure 43. The comparison between the column interaction diagram and the axial loads and moments of the column for Richmond, VA. The points are the factored axial loads and moments in the columns.

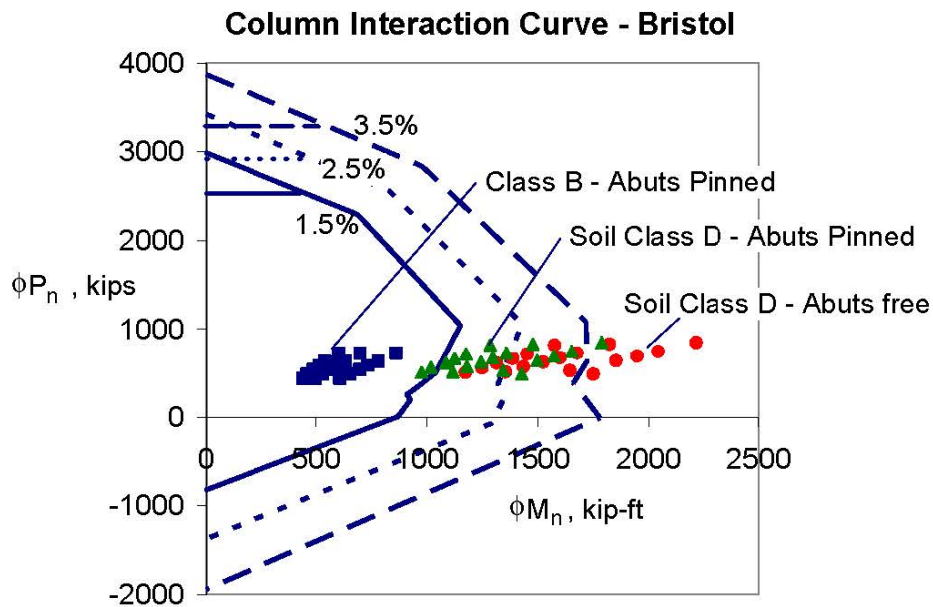


Figure 44. The comparison between the column interaction diagram and the axial loads and moments of the column for Bristol, VA. The points are the factored axial loads and moments in the columns.

For soil class D, the columns for most cases will need to have greater longitudinal reinforcement. In the Vienna area, depending on the degree of fixity at the abutments, 1.5% to 2.5% reinforcement is adequate for all configurations. In the Richmond area, the reinforcement ratio in the columns of bridge with long spans and short columns may need to be increased up to 3.5%. In the Bristol area, column reinforcement may need to be even further increased, or a larger column may need to be used.

Column Transverse Reinforcement

For a circular column to be considered a spiral column, as opposed to a tied column, the *AASHTO LRFD Bridge Design Specifications* in Section 5.7.4.6 require that the ratio of spiral reinforcement to total volume of concrete core be not less than:

$$\rho_s = 0.45 \left(\frac{A_g}{A_c} - 1 \right) \frac{f'_c}{f_{yh}}$$

For this parametric study, assuming an out-to-out spiral dimension of 31 in, the resulting required reinforcement ratio is:

$$\rho_s = 0.45 \left(\frac{1018 \text{ in}^2}{755 \text{ in}^2} - 1 \right) \frac{3.6 \text{ ksi}}{60 \text{ ksi}} = 0.0094$$

A No. 5 spiral at a 4 in pitch results in $\rho_s=0.010$, which meets the above requirement. This transverse reinforcing can then be compared to the detailing requirements of the *LRFD Guidelines*. Sample calculations, presented in Appendix III for worst cases in the study, indicate that this amount of transverse reinforcement will be adequate to meet the seismic requirements in all cases in which a 2.5% reinforcement ratio or smaller will suffice for the longitudinal reinforcing. If a longitudinal reinforcement ratio of 3.5% is required, the transverse reinforcing must also be increased to a No. 6 spiral at a 4 in pitch ($\rho_s=0.0142$).

So, for this parametric study, in all areas of the commonwealth, if the bridges are founded on good soil (Class B) and the abutments are considered to be quite stiff laterally, columns initially designed as spiral columns will not require an increase in spiral reinforcing to bring the design of the piers up to the requirements of the *LRFD Guidelines*. The primary change will be to extend the spiral reinforcement into the cap and the footing, to ensure acceptable behavior of the joints.

However, if bridges are founded on a lower classification of soil (Class D), and the abutments are considered to be quite flexible laterally, the resulting column designs will require more longitudinal reinforcing, and for the Bristol area larger columns may be required.

Conclusions from Parametric Study

This parametric study indicates that the *LRFD Guidelines* will not increase the amount of column reinforcing required in typical two-span overpass structures in Virginia if the bridges are

founded on good soil (Class B). Based on a typical longitudinal reinforcement ratio of 1.5%, bridge columns in this study had adequate axial and flexural strength when subjected to earthquake loading if the soil was Class B. For soil Class D, depending on the fixity at the abutment, the column reinforcement may have to be significantly increased. The transverse reinforcement will not need to be increased if the columns were originally designed as spiral columns unless the longitudinal reinforcing ratio is increased to over 3.5%. If they were originally designed as tied columns, the increase in transverse reinforcement will be significant.

This parametric study investigated only two-span structures with sliding bearings at the abutments. For the case where the abutments were fixed against lateral translation, since the superstructures were very stiff transversely, the piers did not significantly affect the response to lateral loads. Multi-span bridges with narrow width will be more influenced by substructure stiffness, and the substructures will attract larger forces in an earthquake event. For the case of pinned abutments, the majority of the lateral loads applied transversely were resisted by the abutments. This indicates that for this type of bridge the bearings at the abutments, as well as the soil and the piles, should be checked for their lateral load carrying capacity.

CONCLUSIONS

Design Effort

- *The amount of time to check a bridge, previously designed, for compliance with the new LRFD Guidelines is approximately two weeks of workdays (80 to 100 hours) if performed by one person. The analyses require a 3D frame analysis software, such as RISA-3D, which was used to do all the analyses in this study. The two-week approximate required time is much longer than the required time to perform a check on a bridge using the Standard Specifications. Most bridges in Virginia fall into Category A in the Standard Specifications, which requires that the bridge be checked for its bearing length, and the connections at the abutments and piers be checked that they can withstand a lateral load equal to at least 20% of the tributary weight. For bridges that belong to Category B, a check using the earthquake force method, which is similar to the uniform load method explained in this report, is required (AASHTO 1996). Thus the Standard Specifications only require a few hours to perform a check on most Virginia bridges, compared to approximately two weeks using the LRFD Guidelines.*

Longitudinal Column Reinforcement

- *If the longitudinal and transverse restraints are not released at the abutments, the bridges are adequate to sustain the design dead, live and earthquake loads. This conclusion is based on the analyses of the two previously designed bridges in the Bristol District. These bridges had integral abutments, so the intermediate pier would not experience earthquake forces about its weak axis. In the transverse direction, the superstructure was so stiff that most of the earthquake load was carried to the abutments, and the intermediate pier picked up only small additional moments and shears.*
- *Bridges on Class B soil, which can depend on some contribution to lateral stiffness from the abutments, are adequate to sustain the design dead, live and earthquake loads. However, the*

distribution of the transverse earthquake forces to the center pier and the abutments is highly dependent on the assumed spring stiffness of the abutment in the transverse direction. This stiffness is a combination of the soil stiffness and the pile stiffness, which in turn is dependent on the assumed point of fixity of the pile. All these parameters require further investigation.

- *For bridges on Class B soil, if the longitudinal restraint at the abutments is released but transverse restraint is provided, columns with typical amounts of longitudinal reinforcing are able to sustain the design dead, live and earthquake loads, as currently designed. This conclusion is based on the parametric study, in which large forces were carried by the intermediate pier about its weak axis. The short-column and long-span bridges are most severely affected because they have shorter periods of vibration, which result in higher spectral accelerations, and therefore larger equivalent earthquake forces. Furthermore, long-span bridges have more dead load from the weight of their long superstructures. However, all bridges studied on Class B soil with 1.5% longitudinal reinforcing had adequate flexural strength.*
- *For bridges on Class D soil, if the longitudinal restraint at the abutments is released and transverse restraint is considered to be somewhere between a pinned and a free condition, column longitudinal reinforcing will need to be increased in most cases to sustain the design dead, live and earthquake loads. This conclusion is also based on the parametric study that indicated that for regions of low seismicity (such as Northern Virginia) column reinforcing may need to be increased to 2.5%, and for regions of moderate seismicity (such as the Richmond area) column reinforcing may need to be increased to 3.5%. In regions of high seismicity (such as the Bristol area) column size may need to be increased as well.*

Detailing Requirements

- *Virginia bridges with columns designed as tied columns will require a significant increase in transverse column reinforcement. The second example bridge had columns designed as tied columns. The transverse reinforcement was a No. 3 spiral at a 10.5 in pitch. To bring the bridge into compliance with the *LRFD Guidelines* the spiral was increased to a No. 5 at 4 in pitch.*
- *Virginia bridges on Class B soil with columns designed as spiral columns will require no increase or only a slight increase in transverse column reinforcement. If columns are originally designed as spiral columns, additional reinforcement required to comply with the *LRFD Guidelines* will not be great. However, the spiral, or other confinement reinforcing, is required to be extended into the pier cap and footing.*
- *Several typical bridge details will require modifications to meet the requirements of the *LRFD Guidelines*. These include:*
 - Column shear reinforcement in potential plastic hinge zones
 - Transverse reinforcement for confinement at plastic hinges
 - Spiral spacing

- Moment resisting connection between members (column/beam and column/footing joints)
- Minimum required horizontal joint shear reinforcement
- Lap splices at the bottom of the column, which are not permitted
- Column joint spiral reinforcement to be carried into the pier cap beam and footing
- Transverse reinforcement in cap beam-to-column joints

Increased Construction Costs

- *The additional construction costs to bring new bridge designs into compliance with the new LRFD Guidelines will be small. For the prestressed concrete girder bridge and the steel girder bridges, the increase of construction cost would be 0.1% and 0.3%, respectively.*

RECOMMENDATIONS

1. VDOT's Structure and Bridge Division should evaluate all new bridge designs for compliance with the *LRFD Guidelines* to ensure that Virginia bridges are not vulnerable to damage or failure, should the maximum expected earthquake occur.
2. VDOT should consider an analysis of existing critical bridges, particularly those on poor soils, in the south western region of the state to determine if retrofits are necessary to ensure acceptable seismic performance.

SUGGESTIONS FOR FURTHER RESEARCH

In performing the analyses of the two bridges and the parametric study, several assumptions were made, which could be verified through field testing. Subjects for further research included:

1. Investigation of the use of a rigid link to connect the superstructure and the substructure for the purpose of obtaining the load that the superstructure imposes on the substructure
2. Investigation of modeling the stiffness of the abutments and the influence of the stiffness on forces in the piers.
3. Investigation of the fixity of the connection between the superstructure and the abutment.
4. Investigation of longer superstructures, such as multi-span viaducts, in which the substructure stiffness has a greater influence on the structural response.
5. Investigation of the effect of including shear deformations in the analysis.
6. Investigation of abutment and bearing design for earthquake loads.

REFERENCES

- AASHTO (1998). *AASHTO LRFD Bridge Design Specification, 2nd Edition*. American Association of State Highway and Transportation Officials, Washington, D.C.
- AASHTO (1989). *Standard Specifications for Highway Bridges, 14th ed.* American Association of Highway Transportation Officials, Washington, D.C.
- AASHTO (1992). *Standard Specifications for Highway Bridges, 15th ed.* American Association of Highway Transportation Officials, Washington, D.C.
- AASHTO (1996). *Standard Specifications for Highway Bridges, 16th ed.* American Association of Highway Transportation Officials, Washington, D.C.
- ACI Committee 318 (2002). *Building Code Requirements for Structural Concrete (318-02) and Commentary (318R-02)*. American Concrete Institute, Farmington Hills, MI.
- Barker, R. M., and J. A. Puckett (1997). *Design of Highway Bridges, 1st ed.* John Wiley and Sons, Inc. New York, NY.
- Charney, F.A. (2001). *Fundamentals of Earthquake Engineering, Structural Dynamics and Earthquake Engineering Class Lecture Notes*.
- Dove, J. (2002). Professor of Geotechnical Engineering, personal interview. Blacksburg, VA.
- MCEER (2001). *Recommended LRFD Guidelines for the Seismic Design of Highway Bridges, Part I: Specifications*. Multidisciplinary Center for Earthquake Engineering Research, Buffalo, NY.
- Priestley, M. J. N., F. Seible and G. M. Calvi (1996). *Seismic Design and Retrofit of Bridges, 1st ed.* John Wiley and Sons, Inc., New York, NY.
- USGS (2002). <http://geohazards.cr.usgs.gov> . United States Geological Surveys.
- USGS (2002b). Probabilistic Hazard Lookup by Zip code. <http://eqint.cr.usgs.gov/eq/cgi-bin/zipcode.cgi> . United States Geological Surveys, 6 December 2002
- Virginia Department of Transportation (1993). *Proposed Bridges on Route 19 over Connection Existing Route 19 Tazewell County*. Proj. 6019-092-F07, B612 & B613, Richmond, VA.
- Virginia Department of Transportation (2002). *Route 288 PPTA Project*, Proj. 0288-020-105, B683, Richmond, VA.
- Widjaja, M. A.(2003). *The Influence of the Recommended LRFD Guidelines for the Seismic Design of Highway Bridges on Virginia Bridges*. Unpublished Masters Thesis, VPISU, Blacksburg, VA, online at <http://scholar.lib.vt.edu/theses/available/etd-03122003-194010/>

APPENDIX I
PRESTRESSED CONCRETE GIRDER BRIDGE

Table I-1 Joint Coordinates for RISA 3D Model

Joint Label	X-coordinate, in	Y-coordinate, in	Z-coordinate, in
N1	0.0	337.0	0.0
N2	1492.1	337.0	0.0
N3	2984.3	337.0	0.0
N4	1492.1	249.0	484.3
N5	1492.1	249.0	409.4
N6	1492.1	249.0	204.7
N7	1492.1	249.0	0.0
N8	1492.1	249.0	-204.7
N9	1492.1	249.0	-409.4
N10	1492.1	249.0	-484.3
N11	1492.1	0.0	409.4
N12	1492.1	0.0	204.7
N13	1492.1	0.0	0
N14	1492.1	0.0	-204.7
N15	1492.1	0.0	-409.4

Table I-2 Dead and Live Loads in Columns

Load Type	Axial Load, kips				
	Far Left Column	Near Left Column	Center Column	Near Right Column	Far Right Column
Design Truck	14.6	14.1	14.5	14.1	14.6
Design Tandem	10.1	9.6	9.9	9.6	10.1
Two Design Trucks (TT)	25.7	24.6	25.3	24.6	25.7
Lane Load (LN)	20.1	19.3	19.8	19.3	20.1
Controlling Load	25.7	24.6	25.3	24.6	25.7
Total Live Load Effects (LL)*	127.0	121.7	125.0	121.7	127.0
Dead Load (DL)	742.2	724.4	742.2	724.4	742.2
DL + 0.5 LL	805.7	785.3	804.7	785.3	805.7
P/(F _c A _g)	0.162	0.158	0.161	0.158	0.162
I _e /I _g	0.49	0.49	0.49	0.49	0.49
I _e	74,845 in ⁴				

Notes: $I_g = 152,750 \text{ in}^4$
 $LL = 4 \times 0.65 (0.9 \times TT \times 1.33 + 0.9 \times LN)$
column reinforcement ratio = 2.0%

Note that the live loads when multiplied by the 0.5 load factor contribute approximately 8% of the load to the column. This load increases the effective I, makes the substructure somewhat stiffer, therefore the period of vibration is shorter, the spectral acceleration is higher, the equivalent earthquake force is larger and the substructure attracts a greater percentage of it. So including live load effects is a conservative approach to determining column force effects.

Table I-3 – Combined Dead, Live and Earthquake Loads

	Member	Earthquake Lateral	Earthquake Longitudinal	Dead	Live	Ultimate 40% Lat + 100% Long.	Ultimate, 100% Lat. + 40% Lat.
Axial Load, kips	Pier Cap	0.0	0.0	0.0	0.0	0.0	0.0
	FL Column	41.1	-3.8	742.2	124.5	812	830
	NL Column	56.9	-5.7	724.4	119.3	795	820
	C Column	0	-24.9	742.2	122.6	786	796
	NR Column	-56.9	-5.7	724.4	119.3	765	745
	FR Column	-41.1	-3.8	742.2	124.5	790	775
Moment, kip-ft	Pier Cap	1184	324	1311	243.4	324	2222
	FL Column	584	185	-58	-12.8	154	329
	NL Column	662	185	13	2.7	227	458
	C Column	504	185	0	0	183	340
	NR Column	662	185	-13	-2.7	204	430
	FR Column	584	185	58	12.8	252	456

Notes: All earthquake results from Uniform Load Method

FL – Far Left

NL – Near Left

C – Center

NR – Near Right

FR – Far Right

Load Combination U = EQ/1.5 + DL + LL/2

Ultimate combinations are vector sums of forces in orthogonal directions

APPENDIX II
STEEL GIRDER BRIDGES

Table II-1 Joint Coordinates for RISA 3D Model

Joint Label	X-coordinate, in	Y-coordinate, in	Z-coordinate, in
N1	0.0	308.8	0.0
N2	1191.0	308.8	0.0
N3	2352.0	308.8	0.0
N4	939.9	232.9	332.9
N5	985.1	232.9	273.0
N6	1122.4	232.9	91.0
N7	1191.0	232.9	0.0
N8	1259.6	232.9	-91.0
N9	1396.9	232.9	-273.0
N10	1442.1	232.9	-332.9
N11	985.1	0.0	273.0
N12	1122.4	0.0	91.0
N13	1259.6	0.0	-91.0
N14	1396.9	0.0	-273.0
N15	617.8	322.2	-779.7
N16	1805.8	322.2	-779.7
N17	2961.8	322.2	-779.7
N18	1611.7	245.8	-520.2
N19	1658.5	245.8	-582.6
N20	1805.8	245.8	-779.7
N21	1953.1	245.8	-976.7
N22	1999.8	245.8	-1039.2
N23	1658.5	0.0	-582.6
N24	1805.8	0.0	-779.7
N25	1953.1	0.0	-976.7

Table II-2 Dead and Live Loads in Columns in East Bound Bridge

Load Type	Axial Load, kips			
	Far Left Column	Near Left Column	Near Right Column	Far Right Column
Design Truck	16.8	17.3	17.3	16.8
Design Tandem	11.5	11.8	11.8	11.5
Two Design Trucks (TT)	22.5	23.2	23.2	22.5
Lane Load (LN)	15.4	15.9	15.9	15.4
Controlling Load	22.5	23.2	23.2	22.5
Total Live Load Effects (LL)*	104.0	107.2	107.2	104.0
Dead Load (DL)	261.7	277.1	277.1	261.7
DL + 0.5 LL	313.7	330.7	330.8	313.7
$P/(f'c Ag)$	0.075	0.080	0.080	0.075
I_e/I_g	0.402	0.405	0.405	0.402
I_e	61400 in ⁴	61860 in ⁴	61860 in ⁴	61400 in ⁴

Notes: $I_g = 152,750 \text{ in}^4$
 $LL = 3 \times 0.85 (0.9 \times TT \times 1.33 + 0.9 \times LN)$
 column reinforcement ratio = 1.4%

Table II-3 Dead and Live Loads in Columns in West Bound Bridge

Load Type	Axial Load, kips		
	Left Column	Center Column	Right Column
Design Truck	22.3	24.9	22.3
Design Tandem	15.3	17.0	15.3
Two Design Trucks (TT)	29.8	33.2	29.8
Lane Load (LN)	19.8	22.1	19.8
Controlling Load	29.8	33.2	29.8
Total Live Load Effects (LL)*	106.9	119.3	106.9
Dead Load (DL)	278.7	31.58	278.7
DL + 0.5 LL	332.2	375.5	332.2
$P/(f'c Ag)$	0.080	0.090	0.080
I_e/I_g	0.388	0.393	0.388
I_e	59270 in ⁴	60030 in ⁴	59270 in ⁴

Notes: $I_g = 152,750 \text{ in}^4$
 $LL = 2 \times 1.0 (0.9 \times TT \times 1.33 + 0.9 \times LN)$
 column reinforcement ratio = 1.6%

Table II-4 – Combined Dead, Live and Earthquake Loads for East Bound Bridge

	Member	Earthquake ULM	Earthquake SMSAM	Dead	Live	Ultimate ULM	Ultimate, SMSAM
Axial Load, kips	Pier Cap	0.0	0.0	0.0	0.0	0.0	0.0
	FL Column	-1.2	-1.7	261.7	104.0	312.9	312.6
	NL Column	-3.0	-4.1	277.1	107.2	328.7	328.0
	NR Column	3.0	4.1	277.1	107.2	332.7	333.4
	FR Column	1.2	1.7	261.7	104.0	314.5	314.8
Moment, kip-ft	Pier Cap	27.0	36.9	409.6	176.6	515.9	522.5
	FL Column	15.9	21.8	-4.7	-6.0	2.9	6.8
	NL Column	21.4	29.2	8.0	4.9	24.6	29.9
	NR Column	21.3	29.1	-8.0	-4.9	3.8	9.1
	FR Column	15.8	21.7	4.7	6.0	18.2	22.1

Notes: ULM – Uniform Load Method
 SMSAM – Single Mode Spectral Analysis Method
 FL – Far Left
 NL – Near Left
 NR – Near Right
 FR – Far Right
 Load Combination U = EQ/1.5 + DL + LL/2

Table II-5 – Combined Dead, Live and Earthquake Loads for West Bound Bridge

	Member	Earthquake ULM	Earthquake SMSAM	Dead	Live	Ultimate ULM	Ultimate, SMSAM
Axial Load, kips	Pier Cap	0.0	0.0	0.0	0.0	0.0	0.0
	Left Column	-2.7	-3.7	278.1	107.3	330.0	329.4
	Center Column	0.0	0.0	316.8	120.3	377.0	377.0
	Right Column	2.7	3.7	278.1	107.3	333.6	334.2
Moment, kip-ft	Pier Cap	33.4	45.3	434.5	190.1	551.8	559.7
	Left Column	23.7	32.1	11.4	1.4	27.9	33.5
	Center Column	24.4	33.1	0.0	0.0	16.3	22.1
	Right Column	23.5	31.9	-11.4	-1.4	3.6	9.2

Notes: ULM – Uniform Load Method
 SMSAM – Single Mode Spectral Analysis Method
 Load Combination U = EQ/1.5 + DL + LL/2

APPENDIX III

DETAILING CHECKS FOR PARAMETRIC STUDY

Spiral reinforcement ratio to meet *AASHTO LRFD Bridge Design Specifications* Section 5.7.4.6:

$$\rho_{s \text{ req'd}} = 0.0094$$

Spiral reinforcement ratio provided by a No. 5 spiral at a 4 in. pitch:

$$\rho_s = \frac{4A_s}{Ds} = \frac{4(0.31 \text{ in}^2)}{31 \text{ in} \cdot 4 \text{ in}} = 0.010$$

Check this reinforcing ratio for compliance with *LRFD Guidelines*. The section numbers presented in this appendix correspond to *LRFD Guidelines* section numbers.

8.8.2.3.1 Implicit Shear Detailing Approach

a) In potential plastic hinge zones

$$\rho_v = K_{shape} \Lambda \frac{\rho_\ell f_{su}}{\phi f_{yh}} \frac{A_g}{A_{cc}} (\tan \alpha)(\tan \theta)$$

where: K_{shape} = shape factor = 0.32 for circular sections
 Λ = fixity factor = 1 for fixed-free
 ρ_ℓ = longitudinal reinforcement ratio = 0.015, 0.025 and 0.035
 ϕ = strength reduction factor = 0.85
 f_{su} = ultimate tensile stress of longitudinal reinforcement, can be taken as $1.5f_y$
= $1.5 * 60 \text{ ksi} = 90 \text{ ksi}$
 f_{yh} = yield stress of hoop steel = 60 ksi
 A_g = gross area of column = 1018 in^2
 A_{cc} = area of confined core = 755 in^2

$$\tan \alpha = \frac{D'}{L}$$

D' = center-to-center diameter of longitudinal reinforcement pattern = 30 in
 L = column length (shortest is most critical) = $20 \text{ ft} * 12 \text{ in/ft} = 240 \text{ in}$

$$\tan \alpha = \frac{30 \text{ in}}{240 \text{ in}} = 0.125$$

$$\tan \theta = \left(\frac{1.6 \rho_t A_v}{\Lambda \rho_t A_g} \right)^{0.25}$$

where: A_v = shear area of concrete, which may be taken as $0.8A_g$
 $\rho_t = \rho_s/2 = 0.010/2 = 0.005$

$$\text{For } \rho_t = 1.5\% \quad \tan \theta = \left(\frac{1.6 \cdot 0.015 \cdot 0.8}{1.0 \cdot 0.005} \right)^{0.25} = 1.40$$

$$\text{For } \rho_t = 2.5\% \quad \tan \theta = 1.59$$

$$\text{For } \rho_t = 3.5\% \quad \tan \theta = 1.73$$

substituting all values into the first equation results in:

$$\text{For } \rho_t = 1.5\% \quad \rho_v = 0.32 \cdot 1.0 \cdot \left(\frac{0.015}{0.85} \right) \left(\frac{90 \text{ksi}}{60 \text{ksi}} \right) \left(\frac{1018 \text{in}^2}{755 \text{in}^2} \right) 0.125 \cdot 1.40 = 0.002$$

$$\text{For } \rho_t = 2.5\% \quad \rho_v = 0.0038$$

$$\text{For } \rho_t = 3.5\% \quad \rho_v = 0.0058$$

the provided $\rho_v = 0.010/2 = 0.005$, therefore this check is **GOOD** for $\rho_t = 1.5\%$ and 2.5%
check is **NO GOOD** for $\rho_t = 3.5\%$.

7.8.2.4 Transverse reinforcement for confinement at plastic hinges

a) for circular sections

$$\rho_s = 0.008 \frac{f'_c}{U_{sf}} \left[12 \left(\frac{P_e}{f'_c A_g} + \rho_t \frac{f_y}{f'_c} \right)^2 \left(\frac{A_g}{A_{cc}} \right)^2 - 1 \right]$$

where: f'_c = 28 day compressive strength = 3.6 ksi

P_e = factored axial loads including seismic effects (maximum is critical)
= 630 kips (from Widjaja (2003))

U_{sf} = strain energy capacity of transverse reinforcement, can be taken as 16 ksi

for Class B soils ($\rho_t = 1.5\%$):

$$\rho_s = 0.008 \left(\frac{3.6 \text{ksi}}{16 \text{ksi}} \right) \left[12 \left(\frac{725 \text{kips}}{3.6 \text{ksi} \cdot 1018 \text{in}^2} + 0.015 \left(\frac{60 \text{ksi}}{3.6 \text{ksi}} \right) \right)^2 \left(\frac{1018 \text{in}^2}{755 \text{in}^2} \right)^2 - 1 \right] = 0.006$$

the provided $\rho_s = 0.010 \geq 0.006$, therefore this check is **GOOD**.

for Class D soils with pinned abutments ($\rho_\ell = 2.5\%$):

$$\rho_s = 0.008 \left(\frac{3.6 \text{ksi}}{16 \text{ksi}} \right) \left[12 \left(\frac{751 \text{kips}}{3.6 \text{ksi} \cdot 1018 \text{in}^2} + 0.025 \left(\frac{60 \text{ksi}}{3.6 \text{ksi}} \right) \right)^2 \left(\frac{1018 \text{in}^2}{755 \text{in}^2} \right)^2 - 1 \right] = 0.0063$$

the provided $\rho_s = 0.010 \geq 0.0063$, therefore this check is **GOOD**.

for Class D soils with free abutments ($\rho_\ell = 3.5\%$):

$$\rho_s = 0.008 \left(\frac{3.6 \text{ksi}}{16 \text{ksi}} \right) \left[12 \left(\frac{845 \text{kips}}{3.6 \text{ksi} \cdot 1018 \text{in}^2} + 0.035 \left(\frac{60 \text{ksi}}{3.6 \text{ksi}} \right) \right)^2 \left(\frac{1018 \text{in}^2}{755 \text{in}^2} \right)^2 - 1 \right] = 0.007$$

the provided $\rho_s = 0.010 \geq 0.007$, therefore this check is **GOOD**.

this section also states:

s = vertical spacing of hoops, not exceeding 4 in within plastic hinge zones

provided spacing is 4 in, therefore this check is **GOOD**.

7.8.2.5 Transverse reinforcement for longitudinal bar restraint in plastic hinges

$$s \leq 6d_b$$

where: d_b = longitudinal bar diameter, assuming No. 9 bar = 1.128 in

$$s \leq 6 * 1.128 \text{ in} = 6.77 \text{ in}$$

provided spacing is 4 in, therefore this check is **GOOD**.